NASA TECHNICAL NOTE

NASA TN D-6543

EXPERIMENTAL EVALUATION OF A PUMP TEST FACILITY WITH CONTROLLED PERTURBATIONS OF INLET FLOW

by William Stevans and Robert J. Blade

Lewis Research Center
Cleveland, Ohio 44135

NATIONAL AERONAUTICS AND SPACE ADMINISTRATION • WASHINGTON, D. C. • NOVEMBER 1971

1. Report No. NASA TN D-6543	2. Government Accession No.	3. Recipient's Catalog No.
4. Title and Subtitle EXPERIMENTAL EVALUATION OF A PUMP TEST FACILITY WITH CONTROLLED PERTURBATIONS OF INLET FLOW		5. Report Date November 1971 6. Performing Organization Code
7. Author(s) William Stevans and Robert J. Blade		8. Performing Organization Report No. E-4476
9. Performing Organization Name and Address Lewis Research Center National Aeronautics and Space Administration Cleveland, Ohio 44135		10. Work Unit No. 720-03 11. Contract or Grant No.
12. Sponsoring Agency Name and Address National Aeronautics and Space Administration Washington, D.C. 20546		13. Type of Report and Period Covered Technical Note 14. Sponsoring Agency Code

15. Supplementary Notes

16. Abstract

A pump test facility to experimentally investigate the relations governing the operation of a pump under periodic fluctuations of inlet pressure and flow is described. The perturbed flow entering the pump is determined by using the acoustical wave equation and accounting for the motion of the test facility. The perturbed flow leaving the pump is determined by using a specially designed multihole orifice plate. The difference between the perturbed flows entering and leaving the pump was identified to be a compliance flow due to the compliance of the pump structure and the water it contained. Data establishing the validity of the measurement methods are presented.

17. Key Words (Suggested by Author(s))	18. Distribution Statement
Pogo Dynamics Pumps Hydraulics Pump dynamics	Unclassified - unlimited

19. Security Classif. (of this report)	20. Security Classif. (of this page)	21. No. of Pages	22. Price*
Unclassified	Unclassified	49	$3.00

* For sale by the National Technical Information Service, Springfield, Virginia 22151

EXPERIMENTAL EVALUATION OF A PUMP TEST FACILITY WITH CONTROLLED PERTURBATIONS OF INLET FLOW

by William Stevans and Robert J. Blade

Lewis Research Center

SUMMARY

A description of a pump dynamics test facility and the results of its experimental evaluation are presented. The facility is designed to experimentally investigate the relations governing the operation of a pump under periodic fluctuations of inlet pressure and flow. A specially designed throttle produces perturbations to the pump inlet flow and pressure over a frequency range of 2 to 60 hertz. The perturbed flow entering the pump is determined by using the acoustical wave equation to determine the flow in the long inlet line and by accounting for the equivalent vibrational flow due to the longitudinal motion of the inlet line. The perturbed flow leaving the pump is determined by using a specially designed multihole orifice plate.

Independent checks for establishing the validity of the perturbed data are described and applied to the test data. The results indicate that the measurement methods used give reliable values for the perturbed flows and that the motion of the test facility must be accounted for when calculating the perturbed flow entering the pump. Pipe motions of only 7.62×10^{-5} meter (0.003 in.) can result in an error of 100 percent in the flow entering the pump. The difference between the flows entering and leaving the pump was identified as the compliance of the pump structure and the water it contained. The largest volume difference detected was approximately 0.06×10^{-5} cubic meter (0.04 in.^{3}).

An adaptation of the Frahm Vibration Absorber was used to check the vibration flow measurement. The device was found to be effective in reducing the inlet line longitudinal motion for each resonant frequency for which it was set. However, it was effective over only a narrow frequency band about each resonance point and therefore impractical for continuous use over the frequency spectrum covered in the pump tests.

INTRODUCTION

A serious problem in rocket launch vehicle performance is the longitudinal structural oscillation of the vehicle in its fundamental mode, often referred to as "pogo." These longitudinal oscillations are a result of the unstable closed-loop coupling of the vehicle structure and the vehicle propulsion system. The frequency and time of occurrence of the maximum oscillations are different for each type of launch vehicle. For vehicles presently in use, the frequency of these oscillations falls in the range of 5 to 25 hertz. These oscillations usually occur near the end of the boost phase of flight.

The unstable loop coupling of the vehicle structure and propulsion system is self-sustaining and has the following pattern: The structural longitudinal oscillations cause variations in the pressures and flows in the propellant feed systems to the pumps; this results in a variation in the pressures and flows of the propellants delivered to the engine combustion chamber and, hence, in a variation in engine thrust. This variation in engine thrust produces a longitudinal structural oscillation which completes the unstable loop.

Studies of pogo oscillations indicate that it is difficult to write the accurate mathematical transfer function for the performance characteristics of the turbopumps if there is a variation in their inlet pressures and flows. The analytical study of reference 1 represented the turbopump by equations that could be obtained from its steady-state operating characteristics. Two recent experimental investigations to define the turbopump dynamic operating characteristics are reported in references 2 and 3. In these studies certain assumptions or restrictions were placed on the terms of the pump transfer function which prevented obtaining an expression in its most general form.

In order to obtain the pump transfer function in its general form, a experimental study of pump dynamics was undertaken at NASA Lewis Research Center. To conduct these studies a research test facility was constructed which would allow detailed measurements of the fluctuations of pressure and flow at the inlet and exit of the pump.

This report describes the general considerations applied to the design of the test facility, gives specific details of its major components, and presents data which demonstrate that the necessary measurements to permit analysis of pump dynamic characteristics can be made in this facility.

APPROACH

In this experimental evaluation of pump performance with perturbations to the pump inlet conditions, there are two areas of primary interest. The first is the determination of pump resistance and gain terms which are obtained under both noncavitating and

cavitating conditions of pump operation. The second is the determination of the compliance characteristics associated with the pump operating in a cavitating mode.

For facility design purposes the analytical representation of the pump was considered to have the following form:

$$P_d = (1 + A)P_s - BQ_d \tag{1}$$

This expression relates the perturbed inlet pressure P_s and the perturbed discharge pressure P_d to the perturbed outlet flow rate Q_d. The perturbed pressures and flows are periodic sinusoidal variations about the mean value of the respective parameters. The terms A and B are considered to be representative of the pump gain and impedance, respectively, and can be complex values.

When the analytical representation of the pump is of the form of equation (1), there are several different methods of establishing values for the terms A and B. A number of methods were evaluated and the following is the method used in the experimental investigation conducted in this test facility. It was chosen because it permits a solution for unique values of terms A and B. Inspection of equation (1) indicates that for noncavitating operating conditions of the pump, where term A is assumed to be zero, unique solutions for term B can be obtained by using a single set of dynamic test data.

For cavitating operating conditions of the pump, both A and B are unknown; this precludes obtaining a unique solution for them with a single set of dynamic data. For this situation, two sets of dynamic data must be obtained while the pump is operating at the same steady-state operating conditions. Rewriting equation (1) in the following form indicates a method by which this may be accomplished:

$$P_d = (1 + A)P_s - BQ_d = ZQ_d \tag{2}$$

where Z is the hydraulic impedance at the outlet of the test pump. By changing the value of Z, two sets of data in which A and B are unknown can be obtained. This allows for the solution of equation (2) by the method of simultaneous equations and the obtaining of unique values for A and B. Changes in the value of Z, with the pump operating at the same steady-state conditions for both Z values, can be obtained by using orifice plates of different pressure drops at the pump outlet. To maintain the same steady-state operating conditions of the pump with different orifice plate pressure drops, the overall pump outlet pressure drop must be adjusted. This can be accomplished by adjusting a valve, which is placed downstream of the orifice plate, so the same overall steady-state outlet pressure drop exists for both orifice conditions.

The second objective of this experimental evaluation of pump performance with perturbed inlet conditions is the determination of the compliance characteristics associated

with the pump when it is operating with cavitation at its inlet. The determination of the compliance characteristics is based on the measurement of a compliance flow which is the difference between the perturbed flows entering and leaving the pump. This relation can be expressed by an equation of the following form:

$$Q_s - Q_d = EP_s \tag{3}$$

where E is a measure of the compliance.

The methods that were used to measure the perturbed flows required in this investigation were suggested by experience gained in the line dynamics work at this laboratory (refs. 4 and 5). The use of these measuring methods has a significant effect on the configuration of the test facility.

TEST FACILITY

The Lewis Pump Perturbations Test Facility, shown schematically in figure 1, is a closed-loop system containing approximately 9.5 cubic meters (2500 gal) of conditioned water. The facility is an adaptation to the major components of the Lewis Water Tunnel. The components of the Lewis Water Tunnel are the drive system, the water conditioning system, and the mean flow measurement system, all of which are described in reference 6. The components added for the Perturbations Test Facility are the inlet and outlet dynamic flow measurement systems, the inlet and outlet isolation tanks, the inlet flow and pressure perturbing system, the inlet line vibration absorber, and the test pump. Included as an integral part of these items are the dynamic and steady-state instrumentation.

Test Pump

The pump impeller selected for these tests was the unshrouded centrifugal impeller which is shown in figure 2. The pump was designed to operate in the Lewis Water Tunnel, and data on its steady-state performance are given in reference 7.

Dynamic Flow Measurement Systems

The first flow of interest is the flow entering the pump. This flow is determined by measuring the flow in the inlet line approaching the pump and subtracting the equivalent

flow due to the motion of the inlet line. The perturbed flow approaching the test pump was measured by applying the acoustical wave equation to measurements of pressure fluctuations in a long hydraulic line. Detailed derivations of the equations used are given in the appendix of reference 4. The use of this method of measurement requires that the inlet system be of sufficient length (1) to allow calculation of the flow at the pump at low test frequencies, and (2) to allow accurate determination of the acoustic velocity of the fluid at the maximum test frequency (see appendix B for a derivation of the method of determining the acoustic velocity). The inlet system must also be capable of passing the mean flow required by the test pump with a small pressure loss. Based on these requirements the inlet flow measurement system is a 18.3-meter (60-ft) long pipe of 0.20-meter (8-in.) diameter with a 3.76×10^{-3}-meter (0.148-in.) wall thickness. The pipeline is made in four sections which are flanged and bolted together. The flanged joints are constructed so a smooth continuous internal bore is maintained in the pipeline.

The pressure perturbations in the line are measured with five pressure sensors equally spaced along the bottom of the pipeline (see fig. 1) with the sensor diaphragms flush with the internal bore of the pipe. This placement was made to minimize the chance of error in pressure measurement due to gas being trapped near the region of the sensor's diaphragm. The number of sensors used allows four independent calculations of flow to be made at station 5.

The second flow of interest is the perturbed flow leaving the test pump. This was determined by measuring the perturbed pressure drop across a specially designed multihole orifice plate. Data obtained in the line dynamics work (see table I, ref. 5) indicate that such an orifice plate could be used to measure perturbed flow.

The design of the orifice plate is based on its dynamic impedance having resistive and inertive reactive components. The resistive component is assumed to be the slope of the tangent to the steady-state-pressure-drop-against-flow-rate curve for the orifice plate holes. The reactive component is a function of the inertial mass of the fluid in the orifice plate holes and the equivalent of two Rayleigh end corrections for the holes. The effect of the reactance term is reduced to a practical minimum by resorting to a small hole diameter (1.70×10^{-3} m, or 0.067 in.) and a thin plate (1.27×10^{-3} m, or 0.050 in.). The difference between the reactance achieved and the theoretical minimum was equal to the resolution power of the resolved component indicator.

With this type of orifice plate, an error in the perturbed through-flow will result if periodic flexture of the plate, analogous to oil canning, takes place. In order to minimize this problem, a gridwork support structure was attached to the back of the plate.

Based on the preceding conditions an orifice plate was fabricated (fig. 3) which has 1004 holes of 1.70×10^{-3}-meter (0.067-in.) diameter and which with a pressure drop of 345×10^{3} newton per square meter (50 psi) will pass a mean flow of 0.0631 cubic meter per second (2.23 ft^3/sec). The multihole orifice plate is held between a pair of NASA Orifice Plate Flanges which are located approximately 1.2 meters (4 ft) from the exit of

the pump volute (figs. 1 and 4). The perturbed pressures are measured with two flush-diaphragm pressure sensors mounted on the bottom of the outlet line, one on each side of the orifice plate (fig. 5).

Isolation Tanks

The function of the inlet and outlet isolation tanks is to prevent perturbations of the fluid flow from circumnavigating the test loop and to act as system pressure and fluid level control systems. These tanks are each approximately 2.4 meters (8 ft) high and 1.2 meters (4 ft) in diameter. Each tank contains a nitrogen-gas-filled rubber bladder which fills the upper half of the tank.

Inlet Flow and Pressure Perturbing System

The function of this system is to generate the pressure and flow pulsations entering the test pump. The system is located between the inlet isolation tank and the beginning of the straight inlet line, as shown in figures 1 and 6. The system is composed of two parts: the perturbation throttle and the bypass loop. The function of the perturbation throttle is to generate the periodic fluctuations to the mean flow approaching the test pump. The function of the bypass loop is to allow sufficient flow to bypass the perturbation throttle to maintain the mean flow required by the test pump operating condition.

The electro-hydraulic servo-controlled perturbation throttle (fig. 7), which was designed and fabricated at NASA Lewis Research Center, consists of two multislotted plates, one stationary and the other moving. The flow area, and hence the flow, is varied by changes in the alinement of the slots in the moving and stationary plates. The moving plate is suspended upstream of the stationary plate by four flexure arms which maintain a separation of 5.08×10^{-5} meter (0.002 in.) between the plates, thereby eliminating sliding friction while limiting flow leakage. The moving plate is attached to the hydraulic drive piston shaft which actuates it back and forth across the stationary plate in response to the electro-hydraulic servovalve output. A schematic of the throttle control loop is shown in figure 8.

The throttle as designed has the following characteristics:

(1) A full operating stroke of 4.8×10^{-3} meter (0.19 in.), which results in low acceleration forces and low stroke velocity

(2) The ability to operate at full stroke over a frequency range of 1 to 60 hertz

(3) A total moving weight of 3.3 newtons (0.75 lb), resulting in low acceleration forces

(4) A full open flow area of 18.5×10^{-4} square meter (2.86 $in.^2$) and an approach area of 77.4×10^{-4} square meter (12 $in.^2$), giving a high ratio of approach area to throat area which results in a linear flow relation with respect to position

(5) Approximately balanced, lateral, water pressure forces on the moving plate and its suspension arms, which result in near symmetrical loading on the hydraulic drive piston mechanism

(6) An actuating piston area of 1.3×10^{-4} square meter (0.2 $in.^2$), which with the hydraulic supply pressure of $13\ 789\times10^3$ newtons per square meter (2000 psi) results in a ratio of stall force to moving mass weight of 534 g's (The method of valve actuation results in a dc hysteresis of less than 0.5 percent or 2.45×10^{-5} meter (0.001 in.).)

Several other methods of producing the periodic flow fluctuations were considered but each was found lacking in one or more characteristics. Other perturbing devices considered included the piston perturber, the siren valve, and a hydraulically operated commercial valve. The possibility of physically vibrating the pump was also considered.

Inlet Line Vibration Absorber

Experience in the line dynamics work (ref. 4) indicates that, when using the acoustical wave equation to measure the perturbed flow exiting from a long line, the longitudinal motion of the line must be taken into account. To check the accuracy of the measurements made of the longitudinal vibration velocity of the test facility inlet line, a Frahm Vibration Absorber was installed on the line. Discussions on its principle of operation are given in references 8 and 9.

The vibration absorber installed on the facility, shown in figure 9, consists of a mass and spring assembly. The mass is a 3.6-meter (13-ft) long section of 0.254-meter (10-in.) diameter pipe "weighing" approximately 295 kilograms (650 lbf). The mass pipe is split in half along its length and mounted coaxial with the inlet pipe on linear ball bearings, and is attached to the inlet pipe by eight specially designed spring elements. The linear ball bearing and a typical spring element are shown in detail in figure 9. Because of the requirement that the absorber be effective over a large frequency range, two sets of spring elements of the same configuration were used, where the spring constant of one type of element was $1\frac{1}{2}$ times the spring constant of the other. For proper operation of the absorber, the spring force must be coaxial with the mass. To satisfy this requirement, pairs of diametrically opposite spring elements of like spring constant must be connected. By proper combination of spring elements from both sets, eight specific frequencies covering the range of 23 to 52 hertz could be set.

Instrumentation

Two types of instrumentation were used: one to make dynamic measurements, and another to make steady-state measurements.

Dynamic measurements were made of the pressure perturbations in the test loop and of the longitudinal motion of the inlet line. The dynamic pressure measurements were made with commercial, flush-diaphragm, strain-gage pressure sensors. Ten dynamic pressures were measured: five in the inlet line at stations 1 to 5; and three at the pump, one at the pump inlet and two in the pump scroll (stations 6, 7, and 8, respectively). The other two dynamic pressure measurements were made at either side of the outlet orifice plate (stations 9 and 10). Locations of pressure sensors are indicated in figures 1, 5, and 10. Calibration of each sensor with its associated amplifier and power supply was made by using static calibrating procedures. A schematic of the instrumentation signal path and control loop is shown in figure 8.

The longitudinal motion of the inlet line was measured by using two types of motion sensors: a vibration transducer type and a magnet-core - wire-coil type, both units located as shown in figure 10. Both units operate on the principle of electromagnetic induction due to a magnet moving in a coil of wire. However, their construction and method of attachment to the moving item differ. The vibration-transducer-type sensor uses an inertial mass as the reference location, and therefore requires a calibration of the sensor for phase angle over the test frequency range. The magnet-core - wire-coil-type sensor has the coil mounted on a fixed platform and the core mounted on the flange. This setup gives output signal voltages proportional to the velocity of the moving core. For this sensor the manufacturer's calibration was verified; however, it is applicable only when the core is accurately located in the center of the coil. Because of necessary facility maintenance, this condition could not be maintained; therefore, calibration factors were determined by using the vibration transducer sensor each time the facility was disassembled.

The output from the pressure and motion sensors is in the form of an alternating-current electrical signal. The alternating-current signals are amplified and fed into a transfer function analyzer which processes and indicates the data, at any desired reference frequency, in resolved component form. The analyzer effectively rejects all frequencies, noise, and distortion other than the desired reference frequency. The analyzer consists of two units: (1) an oscillator which supplies the signal for the perturbation throttle controller and a four-phase reference voltage for the resolved component indicator, and (2) the resolved component indicator which indicates the in-phase and quadrature components of the data signal with respect to the reference voltage.

Steady-state measurements were made of the steady-state pressure and flow in the pump and test loop and of the rotational speed of the test impeller. The pressure measurements were made with cavity-type, strain-gage, bridge, differential pressure

sensors; each pressure sensor was calibrated by using its associated power supply and a shared switched amplifier. Measurements were made of the pump impeller inlet total pressure, the pump impeller outlet total pressure, and the scroll wall static pressure at the locations indicated in figure 10. Both inlet and outlet total pressure were measured using a claw-type, total-pressure probe set at the mid-passage location. The inlet total-pressure probe was set to the inlet flow angle. The impeller outlet total-pressure probe is mounted in an automatic probe actuator and is alined into the flow stream at each operating point. Both of these pressure measurements were made relative to atmosphere. The wall static pressure in the scroll was measured as a differential with the inlet wall static pressure.

The pressure drop across the outlet orifice plate was measured with a cavity-type pressure sensor and with a precision Bourdon-tube-type gage. Both of these measurements employ pressure taps built into the NASA Orifice Plate Flanges (locations shown in fig. 5).

The mean flow rate was measured with a venturi flowmeter located as shown in figure 1. The pressure drop across the venturi meter was measured with an inverted bifluid manometer using MS 5606 hydraulic oil over water. Both the venturi meter and the multihole orifice plate were calibrated in the system using a single-hole, sharp-edge orifice plate which was located midway along the length of the 18.3-meter (60-ft) inlet line. The single-hole orifice plate was designed to ASME flowmeter standards.

The rotational speed of the pump was measured with a magnetic proximity gage and a 60-tooth steel gear attached to the pump drive shaft. The indication of pump speed was made on an electronic counter.

METHOD OF ANALYSIS

Meaningful results will be obtained from this test facility only if reliable values of the dynamic flows entering and leaving the pump can be determined. This section discusses the methods that are used to make and check these dynamic flow measurements. Details on much of the material in this section are presented in reference 4. For the analysis and equations used in this experimental investigation, it is assumed that analytical stations 1 to 5 are fixed with respect to ground and do not move with the inlet pipe and that stations 6, 6A, 9, and 10 are attached to the pipe (see fig. 1 for station locations).

Inlet Flow Calculation

To obtain the flow at station 5 of the inlet line with respect to ground, the classical one-dimensional wave equation is used in the following form:

$$P_n = P_5 \cos \frac{\omega l_{n-5}}{a} + j \frac{\rho a}{S_5} \left(Q_5\right)_n \sin \frac{\omega l_{n-5}}{a} \tag{4}$$

Using pressures measured at stations 1 to 4 and at station 5, four independent calculations of the $\left(Q_5\right)_n$ flow at station 5 can be made, from which an average Q_5 flow is calculated.

At a frequency where $\sin \omega l/a$ is near zero for a particular calculation, large errors of flow may result from small errors in the measured quantities. At these frequencies the average flow was determined by omitting that particular calculation.

To calculate the flow entering the pump with respect to the pump inlet, the velocity of the pump inlet and pipe combination must be subtracted from the velocity of the fluid. The flow-continuity relation is

$$\frac{Q_{6A}}{S_5} = \frac{Q_5}{S_5} - V_{6A} \tag{5}$$

or

$$Q_{6A} = Q_5 - V_{6A}S_5$$

where Q_{6A} is the flow leaving the 0.20-meter (8-in.) pipe or entering the pump, Q_5 is the flow measured with respect to a fixed reference system, and $V_{6A}S_5$ is the equivalent vibration flow.

A check of the measurement of the equivalent vibration flow can be made by determining the mechanical admittance of the inlet line. To determine the mechanical admittance from experimental data, the driving force tending to vibrate the line in the longitudinal direction has to be obtained. In determining the driving force the following assumptions are made:

(1) Momentum forces resulting from flow direction changes are neglected.

(2) The pressure force at the downstream end of the inlet line is P_5S_5.

(3) The pressure force at the upstream end of the inlet line is P_1S_5, and pressure forces upstream of the end of the 18.3-meter (60-ft) straight pipe are neglected or assumed to be counterbalanced.

The driving force in the flow direction from station 1 to 5 is then

$$F = (P_5 - P_1)S_5 \tag{6}$$

For an ideal viscous-damped, single-lumped spring-mass system, the mechanical impedance is

$$Z_m = \frac{F}{V} = D + j\left(\omega M - \frac{K}{\omega}\right) \tag{7}$$

Hence, the mechanical admittance, which is the reciprocal of the mechanical impedance, is

$$Y_m = \frac{V}{F} = \frac{1}{D + j\left(\omega M - \frac{K}{\omega}\right)} \times \frac{D - j\left(\omega M - \frac{K}{\omega}\right)}{D - j\left(\omega M - \frac{K}{\omega}\right)}$$

$$Y_m = \frac{D - j\left(\omega M - \frac{K}{\omega}\right)}{D^2 + \left(\omega M - \frac{K}{\omega}\right)^2} \tag{8}$$

which yields at resonance $\omega = \omega_o = \sqrt{K/M}$

$$Y_m = \frac{V}{F} = \frac{1}{D} \tag{8a}$$

The mass and spring constant can be determined as follows:

$$\left.\frac{dZ_m}{d\omega}\right|_y = M + \frac{K}{\omega^2} \tag{8b}$$

at resonance

$$\left.\frac{\Delta Z_m}{\Delta\omega}\right|_y = 2M = \frac{2K}{\omega_o^2} \tag{8c}$$

Hence, knowing $\Delta Z_m/\Delta\omega\big|_y$ at $\omega = \omega_o$, the mass and spring constant of the system can be determined from the experimental data. The mass and spring constant of the system can also be determined from static tests. Based on the preceding, two indicators of the quality of the measurements of pressure and velocity (equivalent vibration flow) are

(1) The agreement of the experimental dynamic values of mechanical admittance of the inlet line with the theoretical values determined by using equation (8), where the constants D, M, and K are determined by using equations (7) and (8c)

(2) The agreement of the experimental values of mass and spring constant with the statically determined values of the same parameters

Outlet Flow Calculation

The outlet flow is determined by measuring the pressure difference across the multihole orifice plate. This pressure difference is composed of two parts: the pressure drop associated with the energy loss due mainly to the sudden expansion at the orifice exit, and the pressure difference required to accelerate the mass of fluid between the two measuring stations. The pressure drop due to energy loss is proportional to the flow rate through the orifice and hence is proportional with respect to the orifice, if a linearized equation is used; that is, R_{or} is the slope of the mean pressure drop against mean flow rate. The pressure difference due to acceleration is proportional to the flow with respect to a fixed reference system. Hence, the pressure difference from location 9 to location 10 can be expressed as

$$P_9 - P_{10} = Q_{or}R_{or} + j\omega L_{9\text{-}10}\left(\frac{Q_{or} + V_9S_9}{Q_{or}}\right)Q_{or} \tag{9}$$

where

$$L_{9\text{-}10} = \frac{\rho l_{9\text{-}10}}{S_9}$$

is the expression for the inertance between locations 9 and 10.

If V_9S_9 is small with respect to Q_{or}, the solution for Q_{or} is simple. Fortunately, the mechanical vibration of the outlet pipe is small because of the following:

(1) The facility structure is considered to be stiffer in the outlet direction than in the inlet direction.

(2) Due to the short length of outlet pipe, the pipe mass is low. This low mass in combination with item (1) gives rise to a high resonant frequency and hence to high mechanical impedance at the operating frequencies.

(3) Because the outlet line is short, the contained fluid mass is low; and therefore the driving accelerative pressure forces are low. The low pressure force and high mechanical impedance result in a low vibration velocity. Therefore, the outlet flow was calculated by using equation (9), where V_9 was assumed to be zero, resulting in the following equation:

$$P_9 - P_{10} = Q_{or}(R_{or} + j\omega L_{9-10}) \tag{9a}$$

To decrease the effect of random data scatter in calculating Q_{or}, the pressure difference $P_9 - P_{10}$ was obtained by averaging two sets of data. For one set P_9 and P_{10} were measured independently, and for the other set the differential pressure was measured directly.

A check of the quality of the outlet flow measurement is indicated by the agreement of the experimentally determined and heuristic values of outlet line inertance, $L_{9\text{-tank}}$ and $L_{10\text{-tank}}$.

The experimental values of outlet line inertance are obtained from the following equations:

$$\left.\frac{P_{9,\,tot}}{Q_{or}}\right|_y = \omega(L_{9-10} + L_{10\text{-tank}}) \tag{10}$$

$$\left.\frac{P_{10,\,tot}}{Q_{or}}\right|_y = \omega L_{10\text{-tank}} \tag{11}$$

where it is assumed

(1) That pipe vibration is zero

(2) That the numerators on the left side of the equations are exactly $P_{9,\,tot} - P_{tank}$ and $P_{10,\,tot} - P_{tank}$, respectively, but for this analysis P_{tank} is equal to zero

(3) That $P_{9,\,tot}$ and $P_{10,\,tot}$ are dynamic total pressures

Dynamic total pressure is defined as the sum of the measured wall static pressure and the kinetic pressure, and is expressed by the following relation which neglects second-order terms:

$$P_{tot} = P_S + \frac{\rho \bar{Q} Q}{S_9^2} \tag{12}$$

The heuristic values of outlet line inertance are obtained from the following equations:

$$L_{9\text{-tank}} = \frac{\rho}{S_9}\left(l_{9\text{-tank}} + \frac{8}{3}\sqrt{\frac{S_9}{\pi^3}}\right) \tag{13}$$

$$L_{10\text{-tank}} = \frac{\rho}{S_9}\left(l_{10\text{-tank}} + \frac{8}{3}\sqrt{\frac{S_9}{\pi^3}}\right) \tag{14}$$

where the second term in the equation is the end correction. This end correction accounts for the small reactance at the end of the outlet pipe "looking" into the outlet tank. The end correction is that for a piston mounted in an infinite wall radiating into free space and is called the Rayleigh end correction. The end correction is an approximation because the physics of the internal assembly of the outlet tank introduces complexities which prevent obtaining a more exact expression. A discussion of the limitations to the derivation of exact expressions is given in the text of reference 10. The end correction is nominally 10 percent of the total inertance.

Compliance Flow

The difference between the measured inlet and outlet flow, expressed as

$$Q_{diff} = Q_{6A} - Q_{or} \tag{15}$$

can be caused either by an error in measurement or by a compliance in the pump.

If the difference in flows is due to a compliance, the following equation, which neglects inertance, gives the relation of the compliance, the compliance flow, and the perturbed total pressure:

$$\frac{P_{6,tot}}{Q_c} = \frac{1}{j\omega c} \tag{16}$$

In this equation it is assumed that a single lumped compliance is acted on by a pressure located nearest the pump inlet. It is recognized that in the actual case the volume change is due to distributed compliance and pressure, but for simplicity the aforementioned conditions will be used. The compliance is the ratio of a volume change to an increase in pressure, where the change in volume is composed of the expansion of the pump case and the compression of the fluid associated with the pump. The pressure at the pump inlet was chosen because it is the obvious choice if the pump is cavitating and a reasonable choice if the pump is not cavitating. The total pressure was arbitrarily chosen instead of the static pressure. The difference between the two was less than 5 percent, or 2° in phase angle.

A general distinction between measuring errors and compliance flow can be made by substituting Q_{diff} from equation (15) for Q_c in equation (16). The degree of agreement of the experimental values of Q_{diff} over the frequency range with the theoretical calculations of phase angle and magnitude of Q_c indicates the degree to which the measured difference between inlet and outlet flow is due to compliance rather than to inaccuracies in flow measurement. The amount of compliance is determined from the mean value obtained from equation (16) using Q_{diff} for Q_c. A check of the value of this compliance can be obtained from a static test, in which the volume change in the pump for a given increase in pressure is measured.

TEST RESULTS AND DISCUSSION

The previous section discussed methods used to indicate the reliability of the perturbed flow values as obtained from measurements of perturbed pressure and inlet pipe movement. This section presents and interprets the measured data and calculated parameters that are used

(1) To establish the general reliability of the dynamic pressures, flows, and pipe movement

(2) To demonstrate operation of certain components

(3) To indicate compliance within the pump

Test Conditions

The tests to check the performance of this test facility were made under the following conditions: The frequency of the perturbations to the pump inlet flow and pressure covered a range of 2 to 60 hertz. The water in the system was deaerated to an air content level of 3 ppm by weight and was maintained at 25.55° C (78° F). The test pump impeller was operated at a rotational speed of 50 revolutions per second. A suction

pressure of 482.63×10^3 newtons per square meter (70 psig) was maintained while the impeller was operating over the mean flow rate range of 0.0299 to 0.0524 cubic meters per second (1.058 to 1.849 ft^3/sec). At these conditions, the range of the perturbed flow approaching the pump inlet was 2.26×10^{-4} to 12.17×10^{-4} cubic meters per second (0.008 to 0.043 ft^3/sec).

Pressure Perturbation Generation and Deduction

The function of the perturbation throttle was to produce a sinusoidal variation of pressure in the inlet line. The relation of the throttle position and the oscillator driving voltage with respect to time is shown in figure 11, which is a composite of oscilloscope trace photographs covering the entire frequency range over which the throttle was normally operated. In each photograph the sweep rate of both traces is the same; this allows phase comparison of the driving voltage and valve position traces. The oscillator driving voltage input to the throttle controller and the sensitivity factors for each trace are constant for the series of photographs. The throttle stroke is representative of the stroke used during the tests.

The traces indicate that the throttle is capable of following a sinusoidal driving signal with slight distortion. They also show that as the frequency is increased the stroke amplitude and phase lag increase. For example, at 60 hertz the stroke amplitude is 31 percent greater than that at 1 hertz, and the phase lag between the throttle position and oscillator driving voltage is 112°, or approximately 1.8° per hertz.

A composite of oscilloscope photographs indicating the signals from the flush-diaphragm pressure sensors is shown in figure 12. The number by each trace indicates the station location of the sensor in the test facility as shown in figure 1. The photographs were taken when the pump was in a highly cavitating steady-state condition, where the inlet pressure was 68.947×10^3 newtons per square meter (10 psig). The frequency of the pressure fluctuation is 20 hertz, and the amplitude scale is the same for all traces. The source of the synchronization signal for all these traces is the oscillator signal; therefore, it is possible to compare the phase relation of the traces. For example, the pressure at station 5 lags the pressure at station 1 by approximately 90°.

All the traces, especially those for stations 1 to 4, indicate a general sinusoidal shape as a result of throttle movement and system response.

In the traces of stations 5 and 6 the peaked upper portions and shallow lower portions indicate the bottoming effect of the cavitation at the pump inlet. This cavitation exhibits the characteristic of increasing compliance with decreasing inlet pressure, where the effect of the cavitation sets the lower limit on the value of the pressures at stations 5 and 6. If the cavitation did not have this characteristic, the shape of traces for stations 5 and 6 would be more sinusoidal. Also the traces for stations 1 to 4 would

be cleaner because of the absence of the reflected waves from the cavitation. This cleaning up of the traces was observed in the noncavitating runs.

Inlet Line Vibration

A photograph of the oscilloscope traces for the vibration transducer and magnetic-core - wire-coil combination is shown in figure 13. The steady-state operating point, the dynamic conditions, and the time base for these traces are the same as for those shown in figure 12. It is indicated in figure 13 that the line vibration approximates a sinusoid of the same frequency as the pressure fluctuations generated in the inlet line. Analysis of the traces for the two instruments shows a phase angle difference of approximately 20° at 20 hertz. This difference is a phase error which is an inherent characteristic of the vibration transducer and agrees with the value obtained in the calibration of the sensor. The accuracy of the vibration velocity as measured by these sensors is discussed in a following section.

Measurement of Perturbed Flows

Inlet flow. - The quality of the perturbed flow measurement at station 5 in the inlet line can be assessed from the plots shown in figures 14 and 15. The ratio of each of the four perturbed flows that can be computed at station 5 to the average of these flows at station 5 is plotted in figure 14. The figure indicates that the bulk of the flow data lies within ± 3 percent of the average flow value over the test frequency range. The deviation of the individual phase angles from the average flow phasor phase angle for the same data is plotted in figure 15. This figure indicates that the bulk of the flows has a deviation band of $\pm 2^{\circ}$ from the average flow angle. It can be inferred from these data that the average flow (as defined in the section METHOD OF ANALYSIS) at any frequency will have a tolerance equal to or less than $\pm 2^{\circ}$ in angle and ± 3 percent in flow. In computing the average values for flow and phase angle, the individual data points marked with tails were not included; for these points, $\sin \omega l/a$ is near zero and they are omitted for the reason discussed in the section METHOD OF ANALYSIS.

Vibration flow (mechanical admittance). - The ability to determine the flow due to the longitudinal vibration of the inlet line can be deduced from the data in figure 16. The figure is a plot of the mechanical admittance of the inlet line, both with and without the vibration absorber attached, as a function of the perturbation frequency. The mechanical admittance is the ratio of the longitudinal velocity to the driving force. The plot shows good agreement between the values of mechanical admittance determined experimentally and those determined using a theoretical relation (eq. (8)). The mass and

spring constant used in equation (8) were obtained from experimental dynamic data and equation (8c).

An additional indication of the reliability of the vibration flow measurements is provided by a comparison of the values for the mass and the spring constant of the test facility inlet structure as determined by two methods: (1) using the experimental dynamic data and equation (8c), and (2) performing static pull tests and weight determinations of the facility components.

The mass values were determined to be 920.875 kilograms (63.1 slugs) for the experimental dynamic data and 980.710 kilograms (67.2 slugs) for the weight determination. The weight determination mass value is an average of two calculations of the mass: one included all the facility components from the inlet tank to and including the pump, and the other included only the components from station 1 to and including the pump. This was done because there is an uncertainty as to which of the components from the tank to station 1 vibrate with the same phase and amplitude as the components from station 1 to the pump.

The spring constant values were determined to be 420.288×10^5 newtons per meter (240 000 lb/in.) for the experimental dynamic data and 520.00×10^5 newtons per meter (297 000 lb/in.) ±12 percent for the static pull test. The static-pull-test spring constant value is an average of several tests in which data were taken in a complete loading and unloading cycle.

The resonant frequency calculated by using the static-pull-test spring constant and the calculated weight determinations gives a value of 36.7 hertz, which is in good agreement with the indicated resonant frequency of 34 hertz shown in figure 16. The experimental data at this frequency indicate an average longitudinal movement of the pipe of only 7.62×10^{-5} meter (0.003 in.) rms.

The agreement of the plots of experimental and theoretical values of mechanical admittance and also the agreement between the mass and spring constant values as determined by two methods indicate the validity of the vibration measurements. Since the equivalent vibration flow is equal to $V_{6A}S_5$, it follows that the calculated vibration flow is also valid.

Data shown in figure 16 also illustrate the effectiveness of the vibration absorber to reduce movement of the inlet line. The dashed lines through the solid data points indicate that these points were taken with a specific combination of springs whose design resonant frequency is indicated on the line. The data with the absorber attached were taken at the same steady-state and perturbed operating conditions as the data of run 1 without the absorber. The marked reduction of admittance with the absorber attached is an indication that the longitudinal vibration of the line was substantially reduced. The frequency span over which a particular combination of spring elements was used is indicated by the dashed curves through the data points. The rapid rise from a minimum

value in a small frequency span indicates that each spring element combination is sharply tuned.

Outlet flow. - The perturbed flow leaving the pump is determined by using equation (9a), which assumes that the vibration velocity of the outlet line is zero and is therefore neglected. An indication of the validity of the outlet perturbed flow measurement can be obtained by comparing the experimental values of outlet line inertance (eqs. (10) and (11)) with the heuristic values (eqs. (13) and (14)). This comparison is given in figure 17 for several noncavitating test runs. Data below 12 hertz have not been included because of the large data scatter caused by the extremely small pressure at station 10. These plots indicate that the experimental values fall into a band which approximates the heuristic values up to 28 hertz. In this frequency interval the mean experimental value is 3 percent higher than the heutristic value. Above 28 hertz the data band rises to a higher value and remains at this value to 52 hertz. The shift in level of the experimental data above 28 hertz is probably due to a change in the radiation impedance at the pipe-to-tank junction. See section METHOD OF ANALYSIS for a discussion of this radiation impedance. In both of the plots shown, the limits of the data band are about ±5 percent of the mean experimental value and remain the same over the entire frequency range.

The consistency of the experimental values for both measuring stations and the good agreement of the mean values to the respective heuristic values indicates that the measurements of perturbed outlet flow are reliable.

Combined flows. - The relation of the inlet, outlet, and vibration flows is illustrated in figures 18 and 19. The magnitude of these flows over the range of perturbation frequency is shown in figure 18. Because these flows are phasor quantities, they cannot be manipulated arithmetically. In figure 18 the first point of interest is the concurrence of the flows into and out of the pump over the entire frequency range. For almost the entire range there is a good match, indicating that the method of accounting for the vibration flow works well. The second point of interest is the magnitude and trend of the vibration flow, which at low frequencies is very small and has little effect on the flow determination into the pump. At a frequency of 18 hertz the vibration flow starts to increase with increasing frequency until its magnitude is equal to the flow calculated at station 5 in the line. Thus, the vibration flow has a marked effect on the determination of the flow entering the pump. It is obvious that if there is no compensation for this vibration flow at frequencies above 18 hertz, determination of the flows into the test pump will be in error. The third point of interest is that over the entire frequency spectrum the outlet flow is consistently larger than the inlet flow. This is significant in that it indicates the presence of a form of storage or compliance within the pump.

The magnitude and phase relation between the various flows is shown in figure 19. The distance from the origin to any point is the magnitude of the flow measured. The angle measured clockwise from the right horizontal abscissa to the magnitude line is the

lag angle of the flow relative to the master oscillator signal. The flow phasor which is the line between the station 5 flow and the pump inlet flow point is the vibration flow. The flow phasor which is the line between the outlet flow point and inlet flow point is the difference flow.

Further corroboration of the validity of the inlet line flow, equivalent vibration flow, and pump outlet flow is presented in figures 19 to 21. It is indicated in figure 19 that the difference flow Q_{diff} is obtained by the phasor subtraction of the equivalent vibration flow and the pump outlet flow from the flow at station 5. Because of the requirement of phasor subtraction, any large error in any of these three flows will show up as an inconsistency in the resultant value of Q_{diff}. The error which does exist in the values of these three flow measurements can be evaluated with figures 20 and 21. A plot of the reactive portion of the difference flow impedance with perturbation frequency is shown in figure 20. The data are from seven test runs covering the steady-state noncavitating operating range of the test pump. The plot shows that the data follow the general trend of a straight line (labeled theoretical curve) with a slope of -1. The plot also indicates that the majority of the data points fall within a band of ±33 percent about the value of the theoretical straight line. The significance of this data band is indicated by the plot of the ratio of the difference flow to the summation of the magnitude of the three measured flows with perturbation frequency shown in figure 21. The data in this figure are from the same test runs as used for figure 20. The plot of figure 21 indicates that the data have systematic variation over the frequency range, with a nominal value of 6 percent. Based on this mean value of 6 percent, a worst case of ±2 percent change in the measured flows will result in a ±33 percent change in the value of Q_{diff} (i. e., 0. 02/0. 06) and, similarly, in a ±33 percent change in the value of $\left|P_6/Q_{diff}\right|_y$, which is the value of the data band shown in figure 20.

The variation of the data with frequency in figure 21 is interesting in that, when the flow ratio is at its lowest values, the largest deviation appears in figure 20. Also shown in figure 20 in the 25- to 35-hertz region is an interesting deviation from the general trend of the data; the deviation is indicated by the dashed line. The exact reason for its existence is not known, but it is speculated that the fluctuation is associated with a resonance of the inlet line and the front face structure of the pump.

Compliance flow. - The phase angle between the difference flow and outlet flow for the data in figure 19 suggests that the difference flow is a compliance flow and not a gross error in measurements. This is further substantiated by the information contained in figures 20 and 22. The slope of -1 for the straight line labeled theoretical curve in figure 20 exhibits the theoretical slope of a compliance as defined by equation (16) when plotted on log-log paper. This suggests that Q_{diff} in equation (15) is a compliance flow. This is corroborated by the data in figure 22, which is a plot of the phase angle of the difference flow impedance with perturbed frequency. The plot shows that the data generally lie within $\pm 10^{\circ}$ of -90°, which is the general characteristic of a compliance.

Since Q_{diff} has both of the general characteristics of a compliance, it can be concluded that Q_{diff} is largely a compliance flow.

In order to make an independent evaluation of the existence and magnitude of the compliance, static-pressure tests were performed on the test pump. The objective of the tests was to determine the compliance of both the pump structure and the volume of water it contained. The data obtained in these static tests give a value for the total compliance of 182.802×10^{-13} meter^5 per newton (3.091×10^{-8} ft^5/lb). This value is for the pump structure and only the water contained in the pump. If the compliance of the volume of water from the exit of the pump to the orifice plate is included, the value of the total theoretical compliance is 300.490×10^{-13} meter^5 per newton (5.081×10^{-8} ft^5/lb). Both of these values are close to and bracket the value of the pump compliance determined from perturbed data, which is 265.953×10^{-13} meter^5 per newton (4.497×10^{-8} ft^5/lb). This suggests that the difference between the perturbed pump inlet and outlet flows is largely a compliance flow. A difference between the static and perturbed test values of compliance is to be expected because the exact perturbed test conditions could not be duplicated in the static tests; that is, the pressure distributions in the pump and the volumes of water were not the same for the static and perturbed tests. Included in the plots of figures 20 and 22 are data points (solid circles) from a test run which had the vibration absorber attached to the test facility. The good agreement of the values of compliance impedance and its phase angle for the data with the vibration absorber attached confirms conclusions previously arrived at from the following facts:

(1) The vibration flow measurements under nonabsorbed operation are valid.

(2) The difference flow is actually a compliance flow and not an error in measurement.

CONCLUDING REMARKS

This report has discussed the general design concepts and preliminary operation of a facility designed to make experimental evaluations of pump performance with imposed perturbations to the pressure and flow at the pump inlet. The results from the preliminary operation of the test facility indicate that the necessary measurements required to obtain the dynamic performance of the pump can be made.

The most significant point of the test is that the methods chosen to measure the three basic perturbed flows yield valid results. The methods involve the measurement of the perturbed pressure drop across a special multihole orifice plate to measure the flow leaving the pump, the use of the acoustical wave equation in a long hydraulic line to measure the flow approaching the pump, and the measurement of the longitudinal velocity of the inlet line to determine the equivalent vibrational flow. The difference of the latter two flows gives the flow entering the pump.

It is indicated that for noncavitating pump operation the difference between the perturbed flow into and out of the pump is a compliance flow. The value of the largest experimental noncavitating compliance determined, a volume change of 6.56×10^{-7} cubic meters (0.04 in.^{3}), was corroborated by the data obtained in static tests of the compliance of the liquid in the pump and the dimensional change in the pump structure.

The data indicate that the longitudinal motion of the inlet line is very important and must be taken into account when using the acoustical wave equation to measure perturbed flows. This was found to be especially important in the region of the point of mechanical resonance of the inlet system. In this region the vibration flow can equal the calculated line flow and hence produce large errors in the evaluation of the dynamic characteristics of the pump if it is not accounted for.

The tests show that the specially designed perturbation throttle was capable of following a sinusoidal driving signal and producing a usable sinusoidal variation of pressure over the frequency range of 2 to 60 hertz.

The preliminary results gained by using the Frahm Vibration Absorber indicate that this type of device can be used to minimize the longitudinal vibration of the test facility. However, this type of device has a narrow frequency range for effective operation.

Based on the experience gained in these tests, careful consideration should be given to the placement of the dynamic pressure sensors in the pump. The pressure sensors should be placed where flow areas can be specifically defined; this will aid in the calculation of the velocity head portion of the total perturbed pressure.

Lewis Research Center,
National Aeronautics and Space Administration,
Cleveland, Ohio, August 13, 1971,
720-03.

APPENDIX A

SYMBOLS

A	pump gain
a	wave velocity, m/sec (ft/sec)
B	pump impedance
c	compliance, m^5/N (ft^5/lb)
D	effective mechanical viscous-damping resistance, N-sec/m (lb-sec/ft)
F	vibromotive force, N (lb) rms, complex
f	frequency, Hz
j	defined by $j^2 = -1$
K	effective mechanical stiffness, N/m (lb/ft)
L	inertance, $N\text{-}sec^2/m^5$ $(lb\text{-}sec^2)/ft^5$
l	length, m (ft)
M	mass, kg (slug)
P	pressure perturbation, N/m^2 (lb/ft^2) rms, complex
Q	volume flow perturbation, m^3/sec (ft^3/sec) rms, complex
$\overline{Q}$	volume flow steady state, m^3/sec (ft^3/sec)
Q_{diff}	defined by eq. (15), m^3/sec (ft^3/sec) rms, complex
R	resistance, $N\text{-}sec/m^5$ ($lb\text{-}sec/ft^5$)
S	cross-sectional flow area, m^2 (ft^2)
V	vibration velocity, m/sec (ft/sec) rms, complex
Y_m	mechanical admittance, m/N-sec (ft/lb-sec), complex
Z	impedance, $N\text{-}sec/m^5$ ($lb\text{-}sec/ft^5$)
Z_m	mechanical impedance, F/V, N-sec/m (lb-sec/ft), complex
ρ	density, kg/m^3 ($slugs/ft^3$)
ω	$2\pi f$

Subscripts:

c	compliance (flow), see eq. (16)
d	discharge

n	location number (1 to 4 as applicable)
o	resonance
or	orifice
s	inlet
tank	outlet tank
tot	total (calculated from the sum of the measured static and the computed dynamic), see eq. (12)
vib	vibration
X	real part of a complex number
Y	imaginary part of a complex number
1-10	locations shown in fig. 1 (Analytical stations 1-5 are attached to ground; analytical stations 6-10 are attached to the pump and pipe.)
6A	see fig. 1

APPENDIX B

EXPERIMENTAL DETERMINATION OF ACOUSTIC VELOCITY

The acoustic velocity of a liquid in a round uniform pipe of known dimensions is easily computed. Because the long inlet pipe in this facility was made up of rolled welded pipe which has normal dimensional variations, an experimental determination of the acoustic velocity of the liquid in this line was made. The acoustic velocity was determined by using a version of the classical Kundt's method. This method involves the solution of the acoustical wave equation (1) to yield the frequency corresponding to a half wavelength in the line. At

$$\frac{\omega l_{1\text{-}5}}{a} = \pi = \frac{2\pi f l_{1\text{-}5}}{a}$$

equation (1) reduces to

$$P_1 = -P_5 \tag{B1}$$

Putting this in complex notation gives

$$P_{1X} + jP_{1Y} = P_{5X} - jP_{5Y} \tag{B2}$$

Equating real and imaginary parts,

$$P_{1X} = -P_{5X} \tag{B3}$$

$$P_{1Y} = -P_{5Y} \tag{B4}$$

Multiplying equation (B3) by equation (B4) yields

$$P_{1X}P_{5Y} = P_{1Y}P_{5X} \tag{B5}$$

Putting these pressure values in terms of their indicator values yields

$$g_1T_XE_{1X}g_5T_YE_{5Y} = g_1T_YE_{1Y}g_5T_XE_{5X} \tag{B6}$$

where

g pickup sensitivity

T indicator sensitivity

E indicator reading

Dividing equation (B6) by $g_1 T_X g_5 T_Y$ yields

$$E_{1X}E_{5Y} = E_{1Y}E_{5X} \tag{B7}$$

The products $E_{1X}E_{5Y}$ and $E_{1Y}E_{5X}$ obtained from several runs were plotted as a function of frequency. The frequency at which the difference of the products goes to zero is used to calculate the acoustic velocity of the liquid in the line. The average value of the experimental acoustic velocity was found to be 1195 meters per second (3919 ft/sec) with an average difference between runs of 5.8 meters per second (19 ft/sec), or 1/2 percent. The theoretical values of acoustic velocity for the dimensional tolerance range of the rolled steel pipe yield values of 1143 to 1207 meters per second (3749 to 3961 ft/sec), which encompass the experimentally determined value.

The simplicity and accuracy of this experimental method, which does not require calibration of either the sensors or indicating apparatus, makes this a desirable means of determining the acoustic velocity of a liquid in a pipeline.

REFERENCES

1. Rubin, S.: Instability Model of Missile Longitudinal Oscillation Due to Propulsion Feedback. Rep. TOR-269 (4126)-28, Aerospace Corp., Sept. 21, 1964. (DDC No. AD-458211.)

2. Anon.: J-2 Vehicle Longitudinal Stability (POGO) Analysis Program. Rep. R-6283, Rocketdyne Div., North American Aviation (NASA CR-71905). Aug. 31, 1965.

3. Bikle, F. E.; Fidler, L. E.; and Rohrs, J. B.: A Study of System Coupled Instability Analysis Techniques. Pts. I and II. Rep. CR-66-36, Martin Co. (AFRPL-TR-66-143, AD-485312 and AD-485313), July 1966.

4. Blade, Robert J.; Lewis, William; and Goodykoontz, Jack H.: Study of a Sinusoidally Perturbed Flow in a Line Including a 90^{o} Elbow with Flexible Supports. NASA TN D-1216, 1962.

5. Holland, Carl M.; Blade, Robert J.; and Dorsch, Robert G.: Attenuation of Sinusoidal Perturbations Superimposed on Laminary Flow of a Liquid in a Long Line. NASA TN D-3099, 1965.

6. Crouse, James E.; Montgomery, John C.; and Soltis, Richard F.: Investigation of the Performance of an Axial Flow Pump Stage Designed by the Blade Element Theory Design and Overall Performance. NASA TN D-591, 1961.

7. Miller, Max J.; and Soltis, Richard F.: Detailed Performance of a Radial-Bladed Centrifugal Pump Impeller in Water. NASA TN D-4613, 1968.

8. Den Hartog, J. P.: Mechanical Vibrations. Fourth ed., McGraw-Hill Book Co., Inc., 1956.

9. Churchill, Ruel V.: Operational Mathematics. Second ed., McGraw-Hill Book Co., Inc., 1958.

10. Lord Rayleigh: Theory of Sound. Second ed., Dover Publications, 1945.

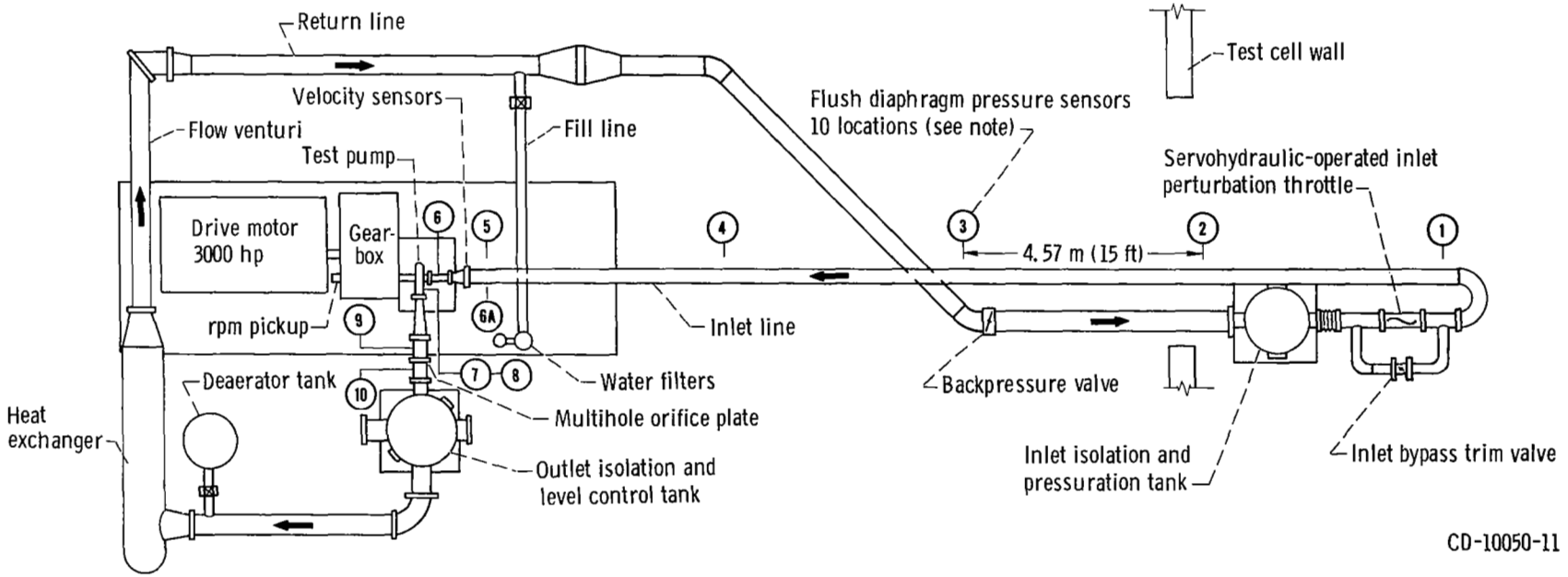

Figure 1. - Pump Perturbations Test Facility, showing analytical reference stations. For analytical purposes stations 1 to 5 and 6A are assumed to be attached to ground; stations 6 to 10 are assumed to be attached to the pump and pipe.

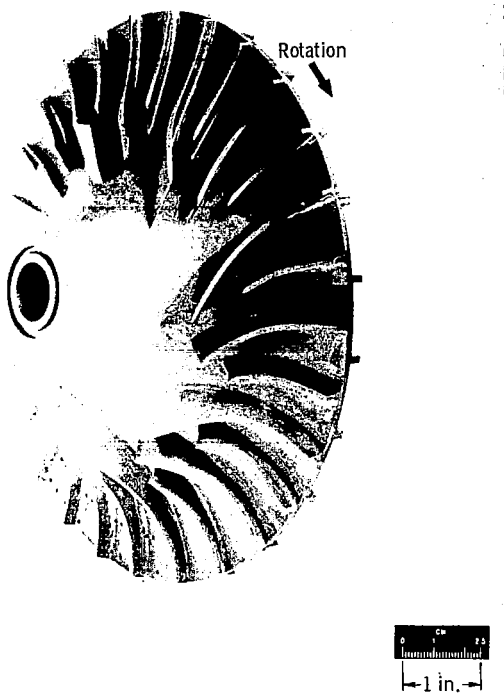

C-67-2902

Figure 2. - Test pump impeller.

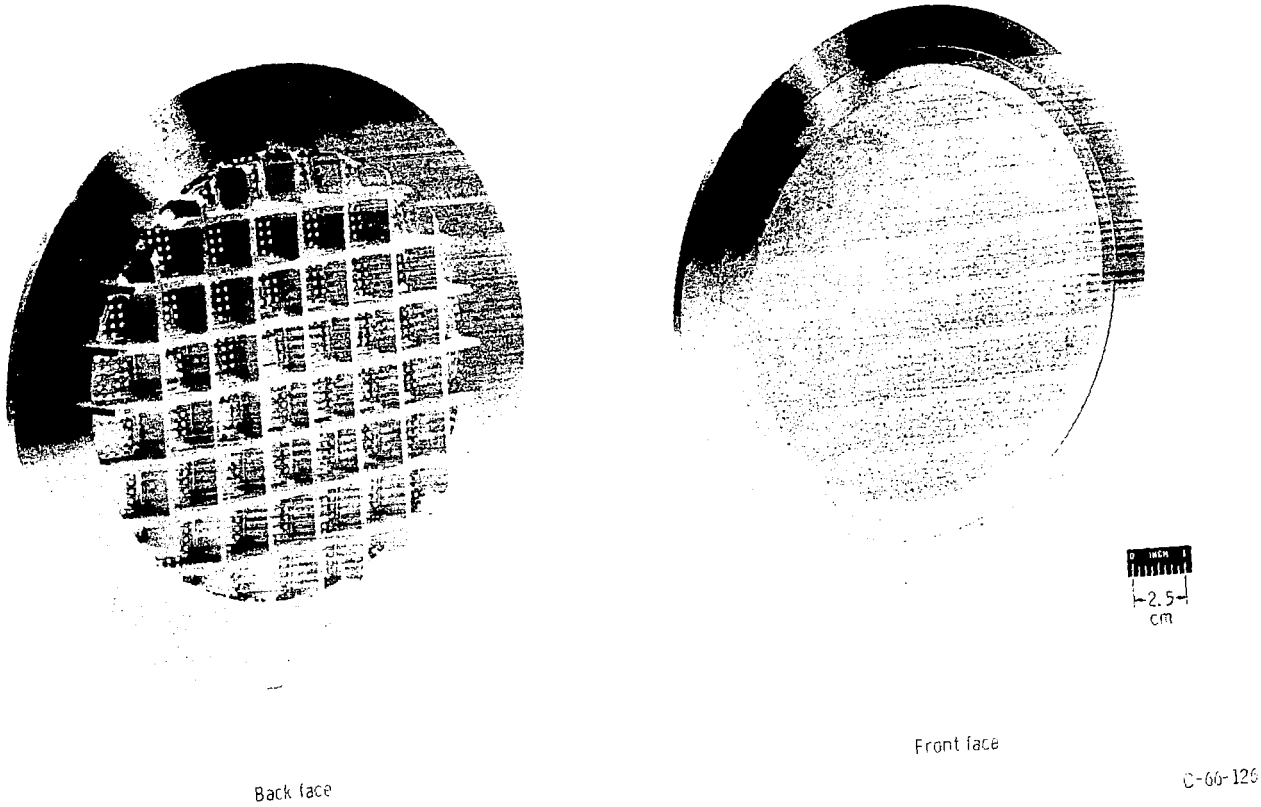

Figure 3. - Multihole orifice plate.

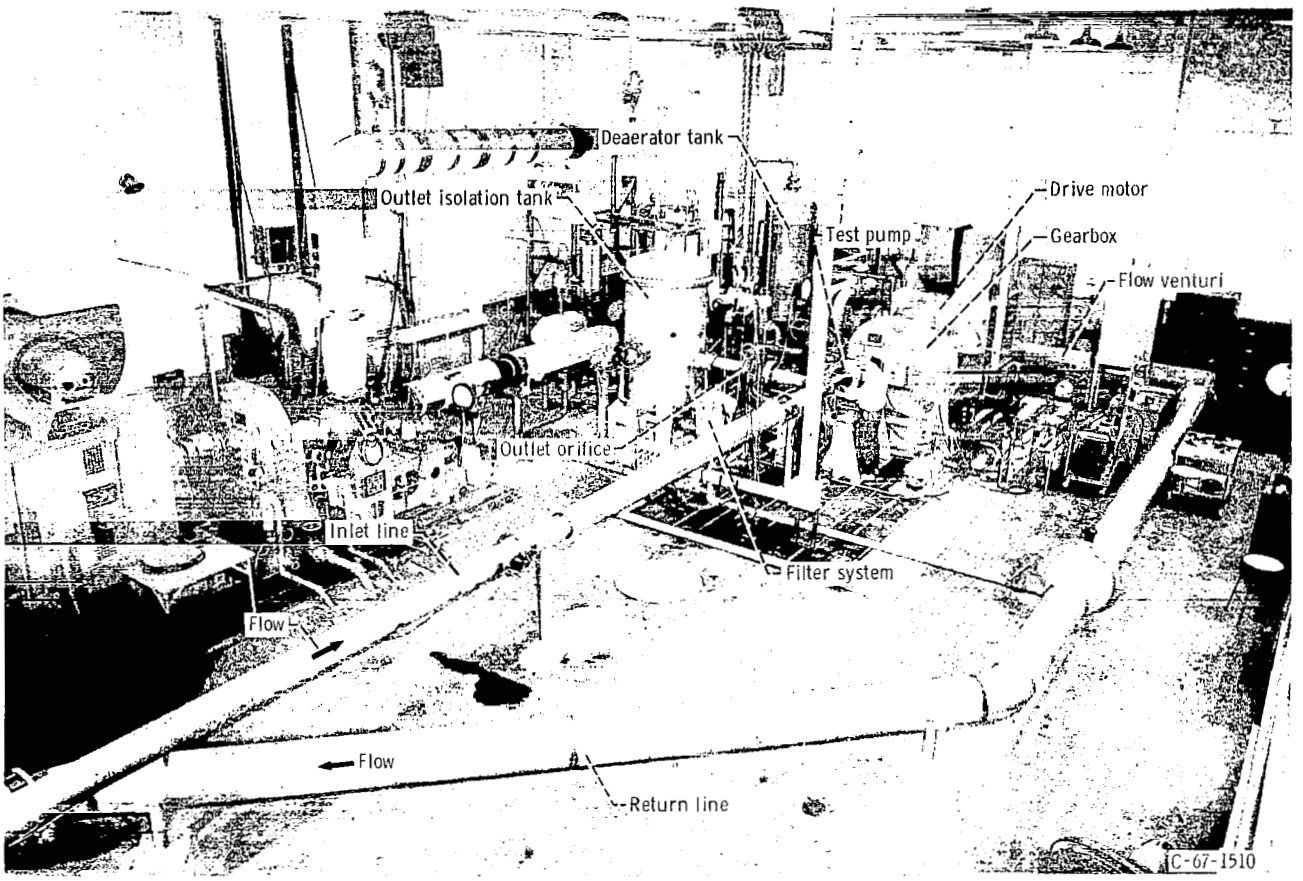

Figure 4. - Pump Perturbations Test Facility - interior of test cell.

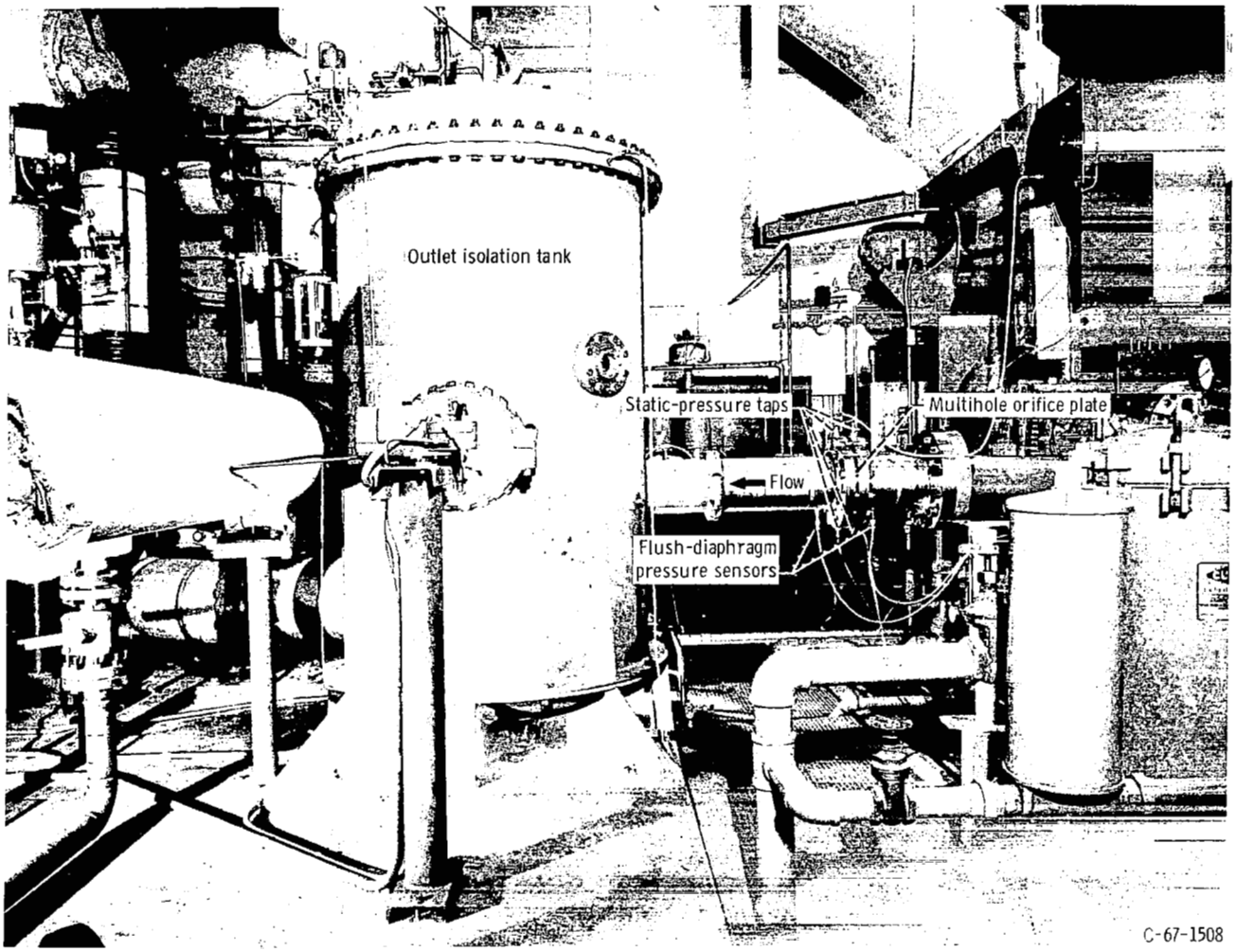

Figure 5. - Exit line, showing multihole orifice plate and pressure sensor locations.

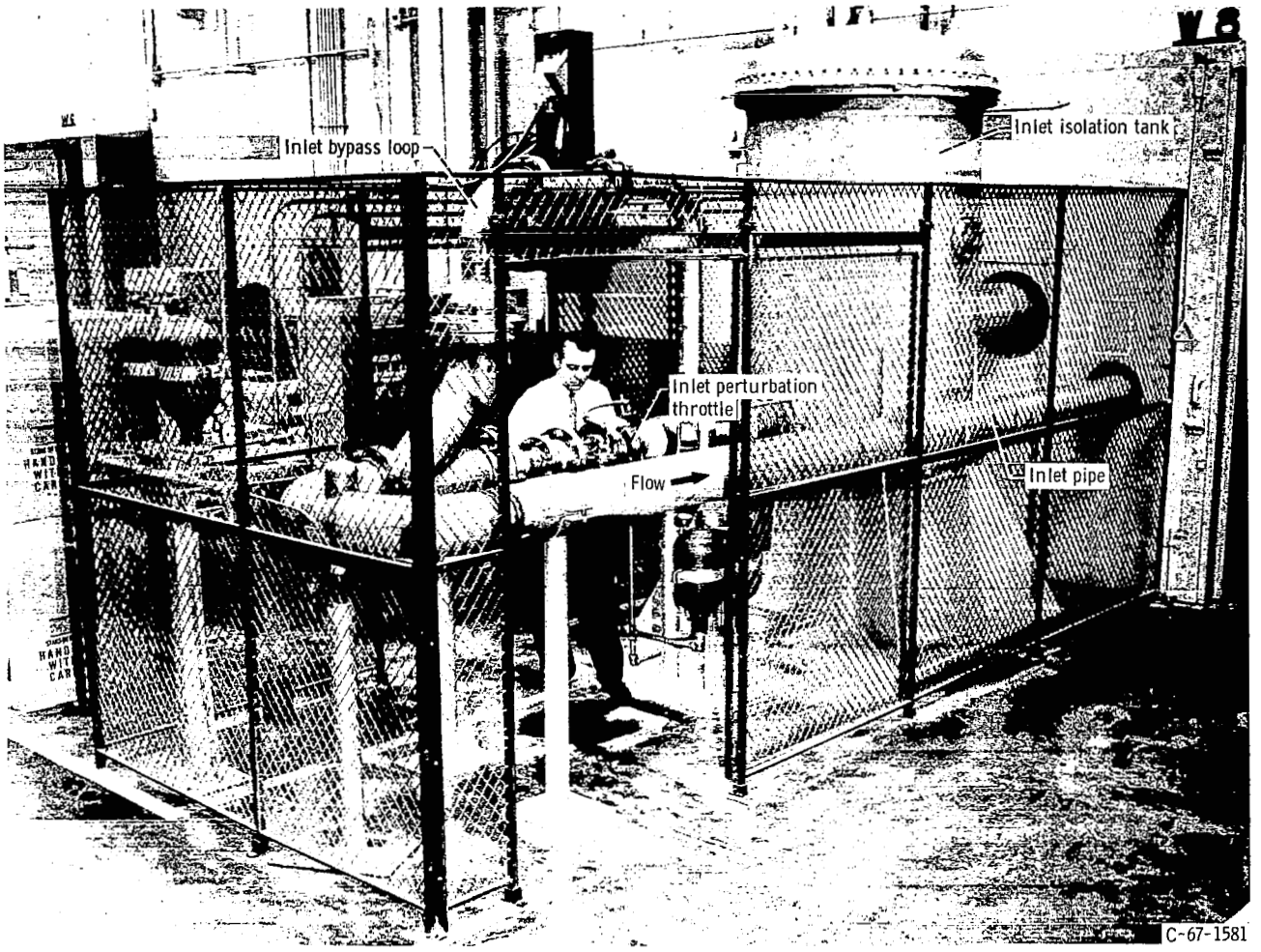

Figure 6. - Inlet flow and pressure perturbing system.

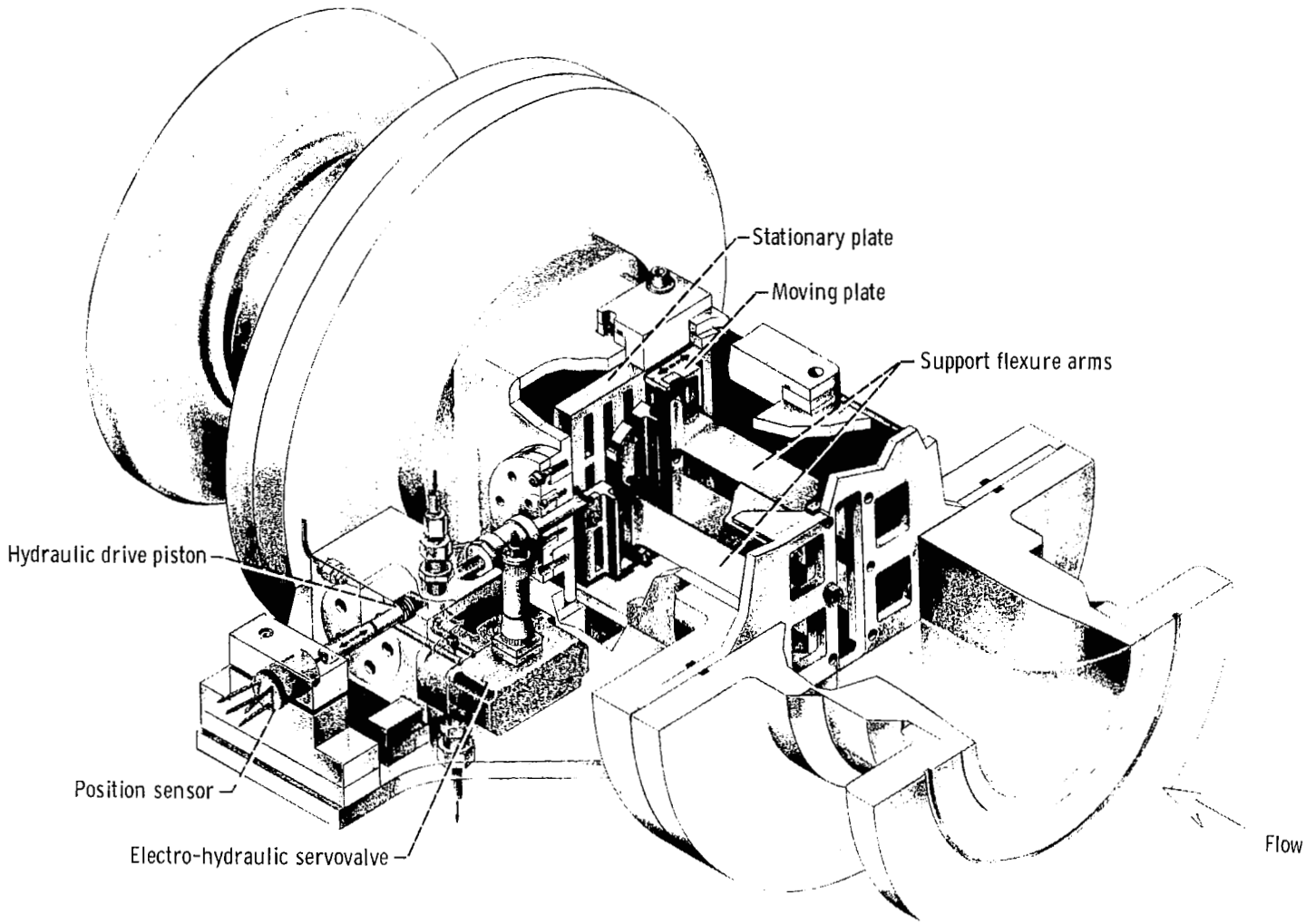

Figure 7. - Perturbation throttle.

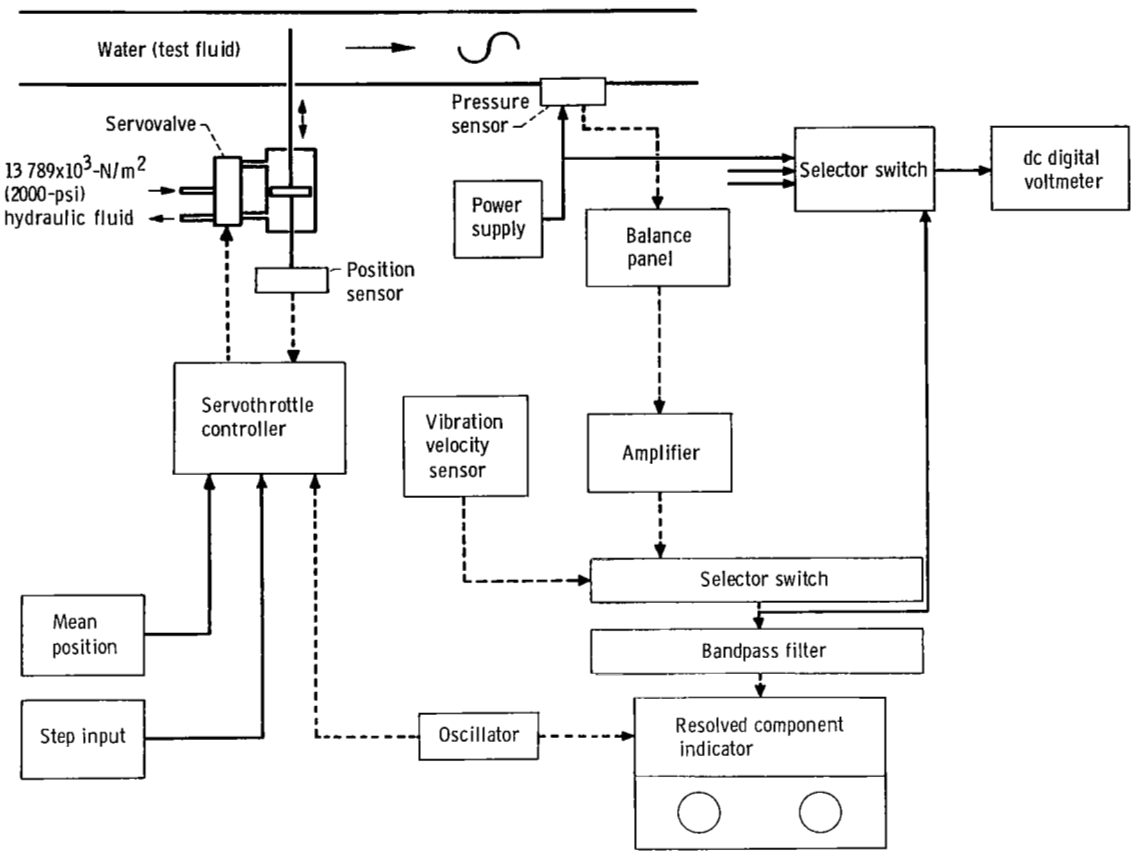

Figure 8. - Control and signal flow sheet. Solid lines indicate dc voltage; dotted lines indicate ac voltage.

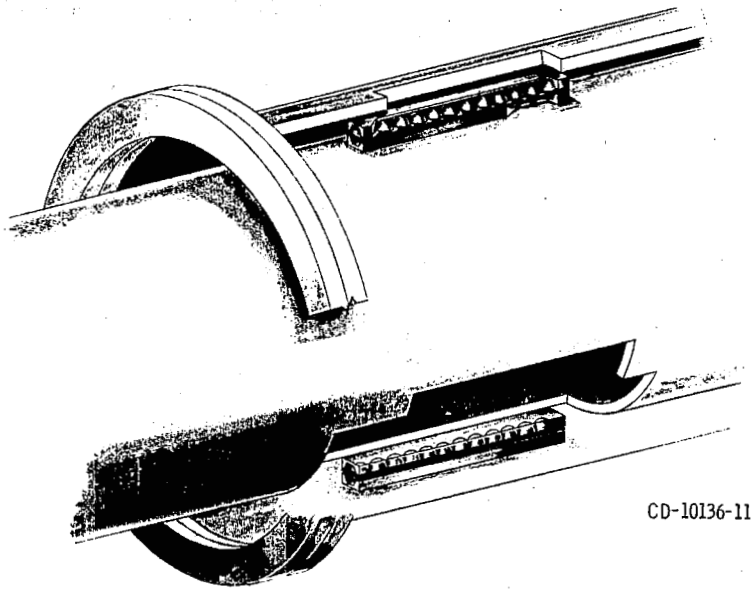

CD-10136-11

Linear ball bearing

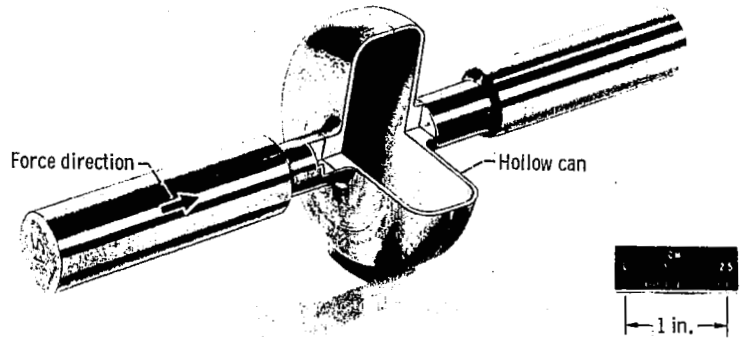

CD-10135-11

Vibration absorber spring element

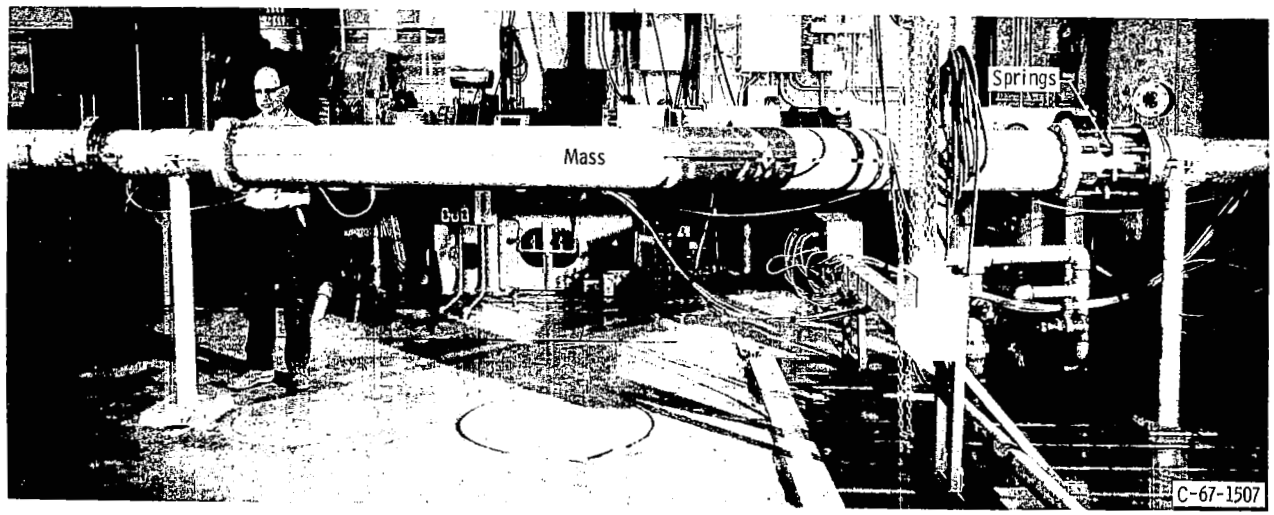

Figure 9. - Vibration absorber with details of linear ball bearing and spring element.

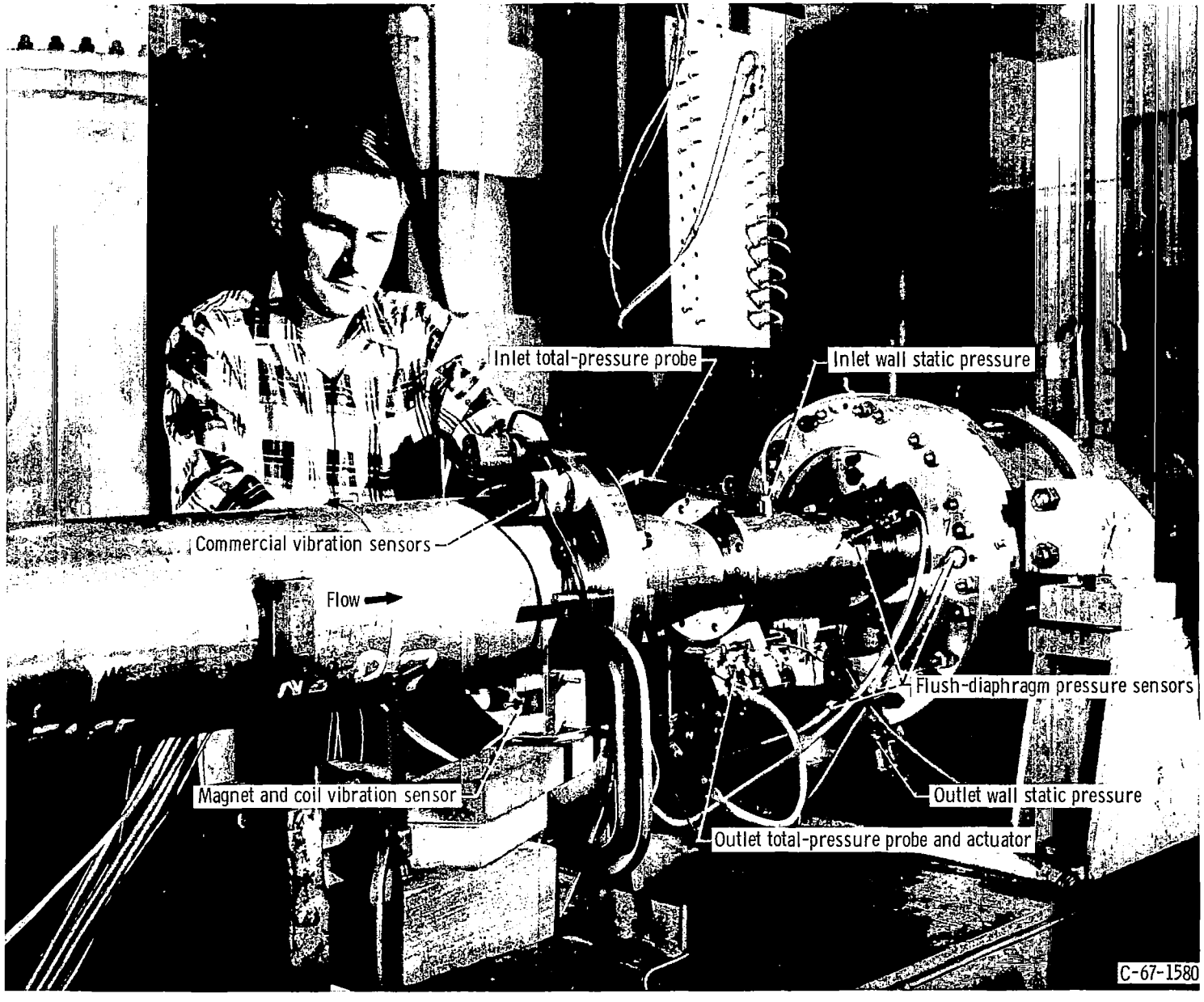

Figure 10. - Test pump and instrumentation.

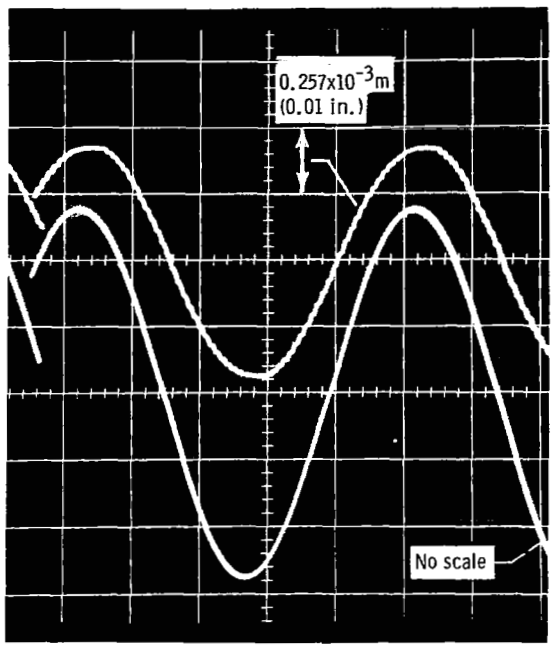

(a) Frequency, 1 hertz.

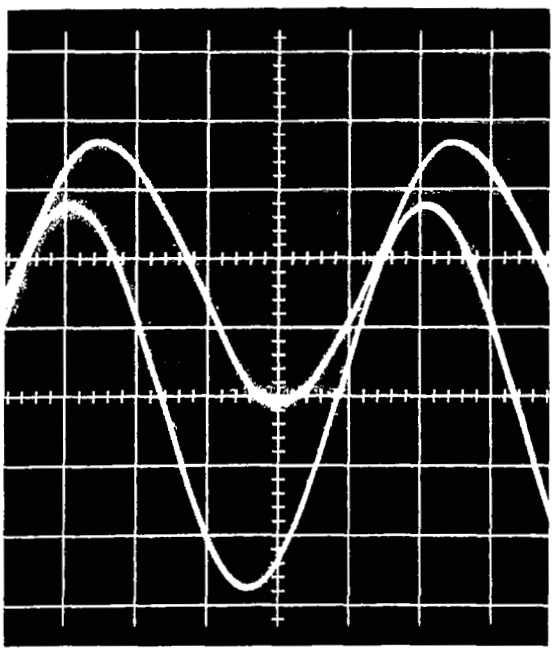

(b) Frequency, 20 hertz.

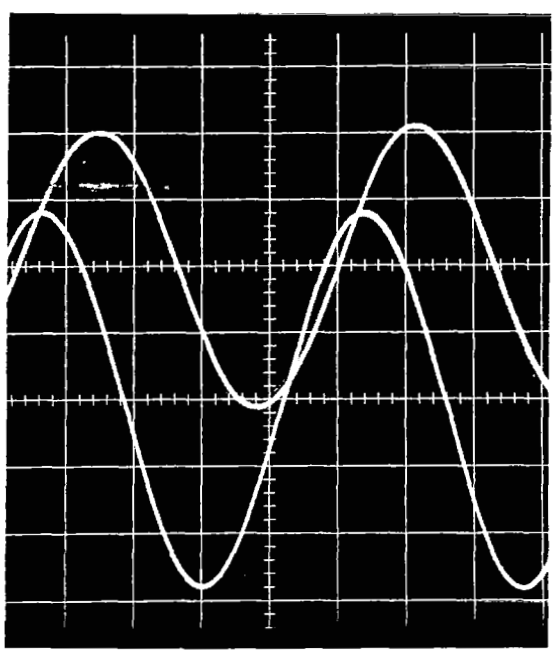

(c) Frequency, 40 hertz.

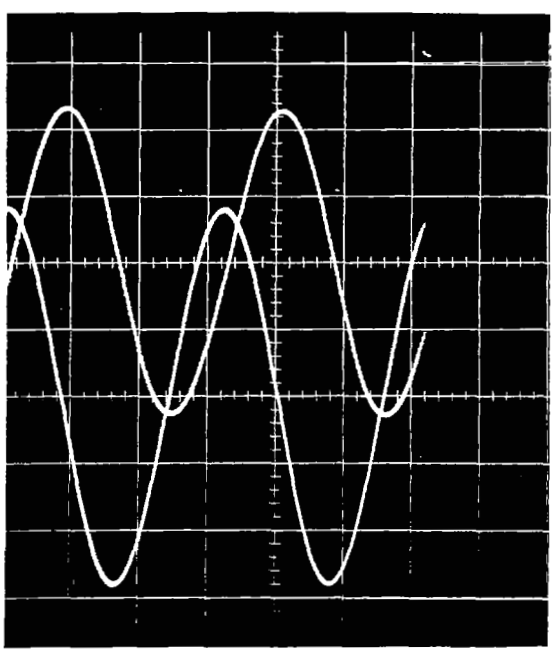

(d) Frequency, 60 hertz.

Figure 11. - Comparison of oscillator drive voltage and valve position. Valve stroke (peak to peak) equals 18.75 percent of full stroke (peak to peak) at 1 hertz. Top trace indicates valve position; bottom trace indicates drive voltage.

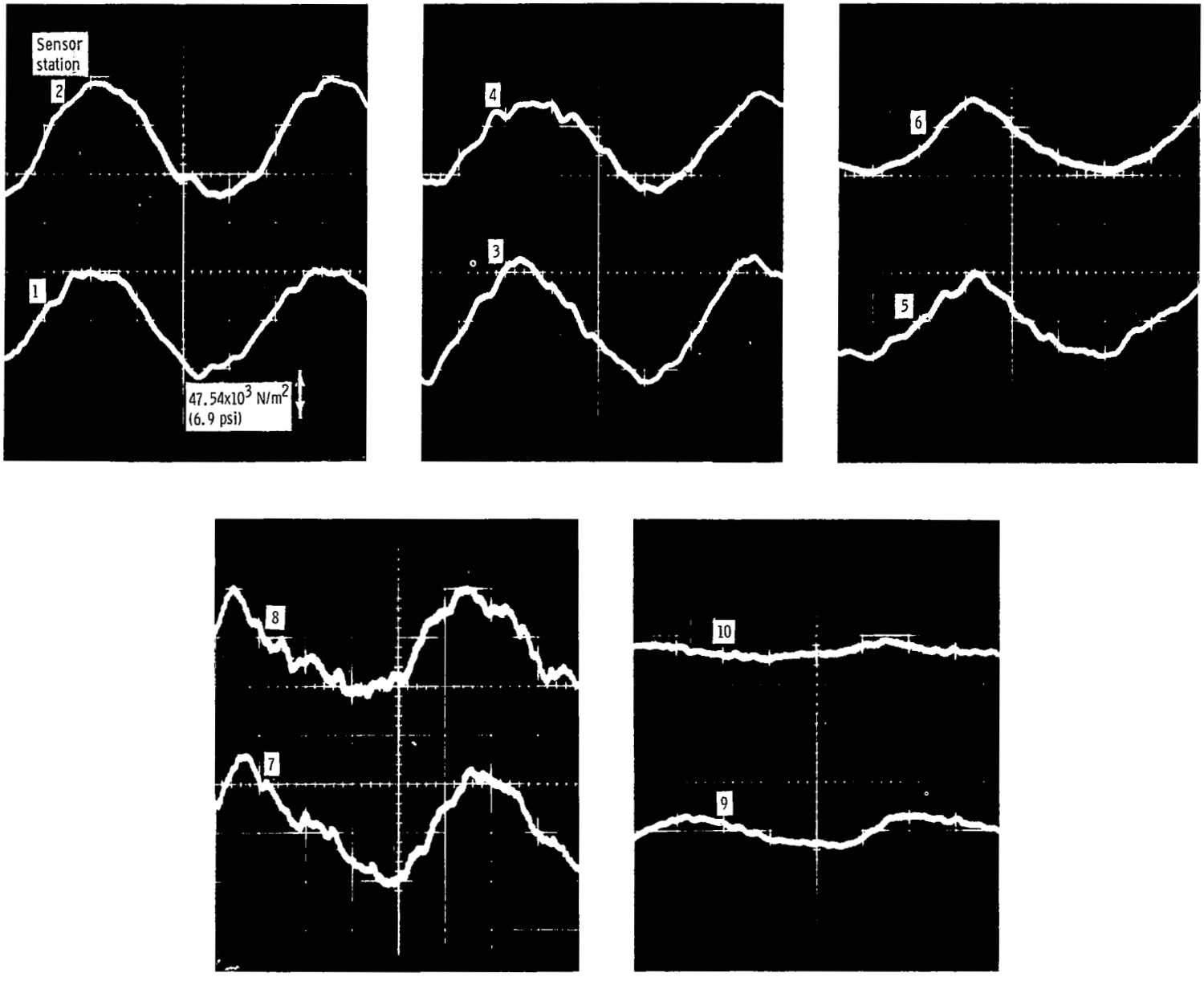

Figure 12. - Pressure sensor traces for various locations. Perturbation frequency, 20 hertz; all traces on same time base.

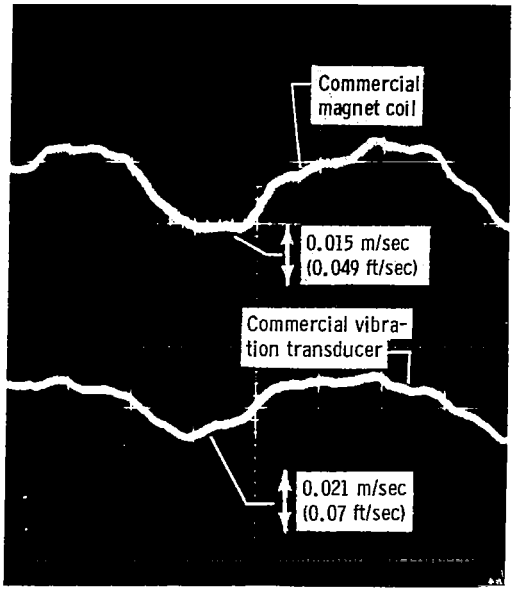

Figure 13. - Inlet line vibration indication. Perturbation frequency, 20 hertz.

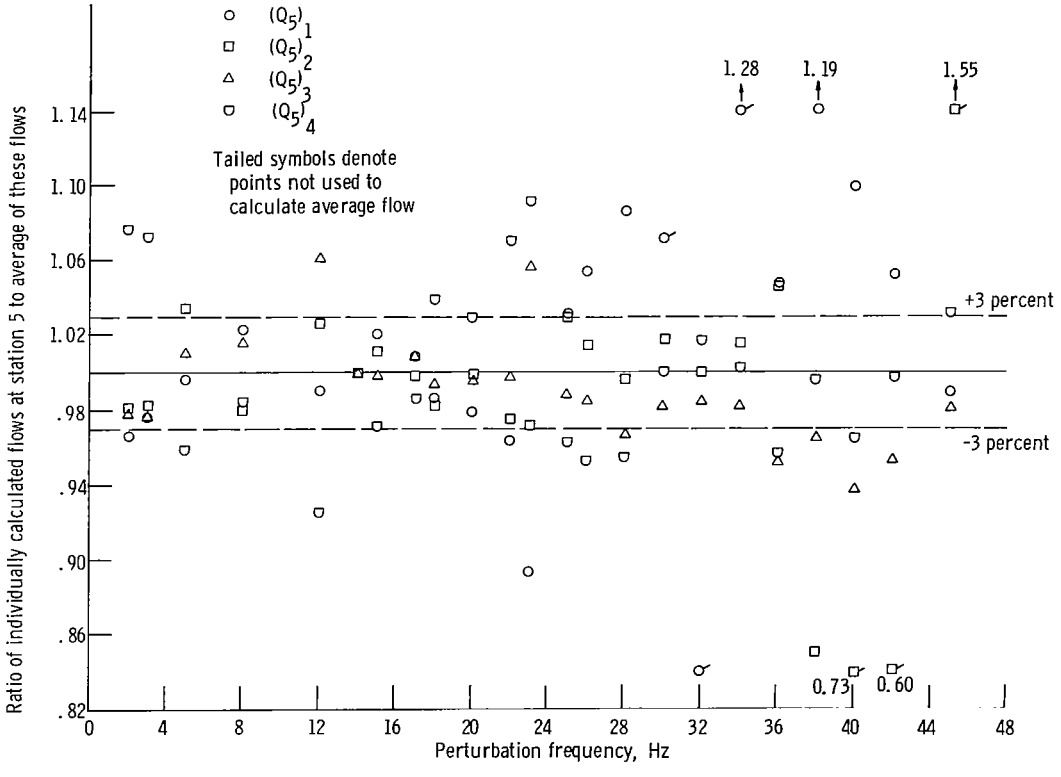

Figure 14. - Ratio of individually calculated flows at station 5 to average of these flows as function of perturbation frequency.

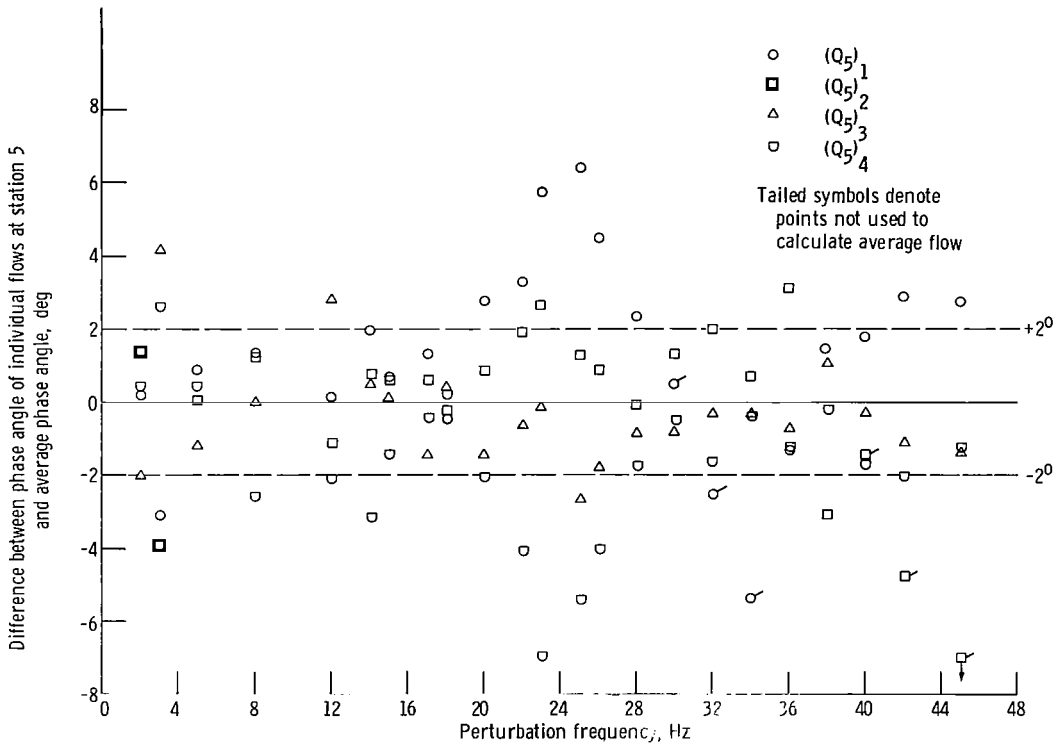

Figure 15. - Difference between phase angle of individual flows at station 5 and average phase angle as function of perturbation frequency.

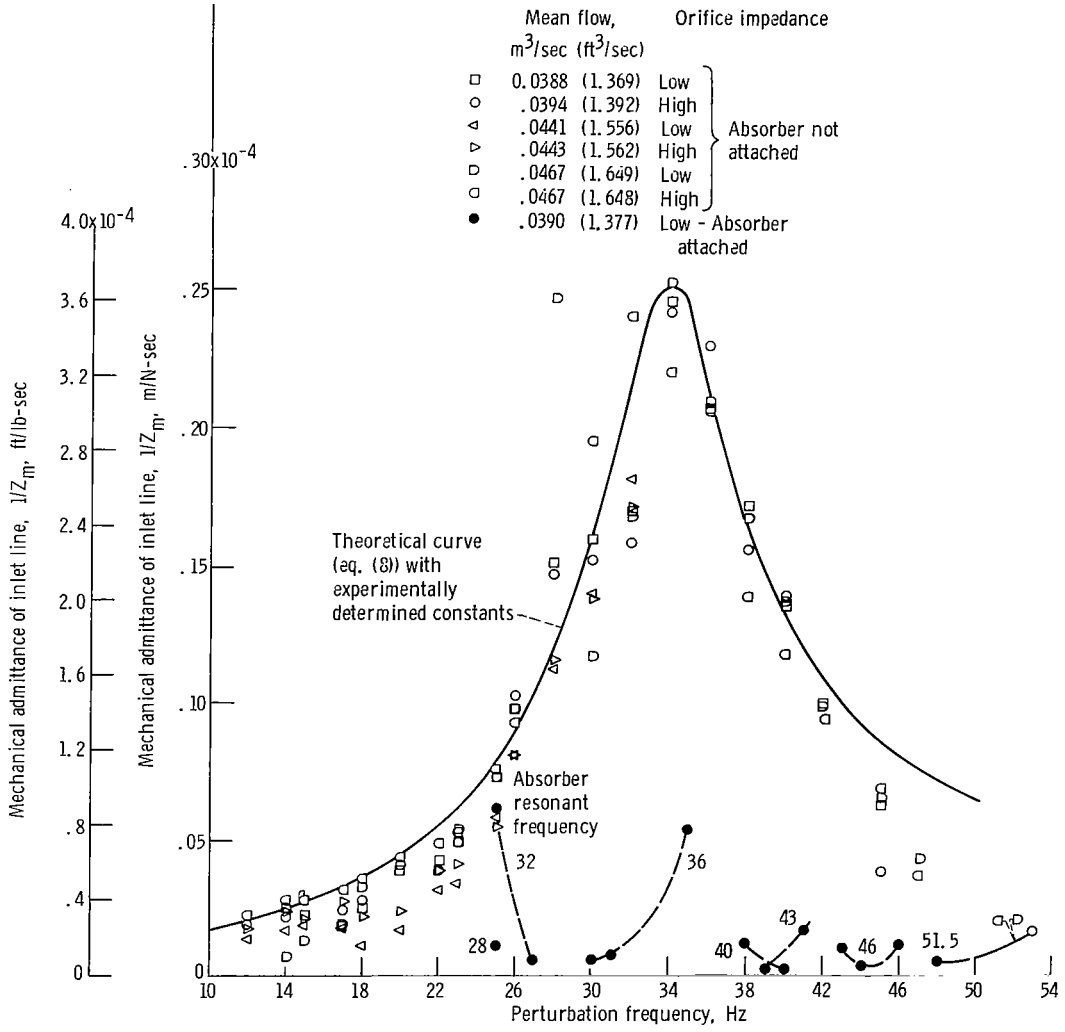

Figure 16. - Mechanical admittance of inlet line as function of perturbation frequency. Pump inlet pressure for all runs, 482.63×10^3 newtons per square meter (70 psi).

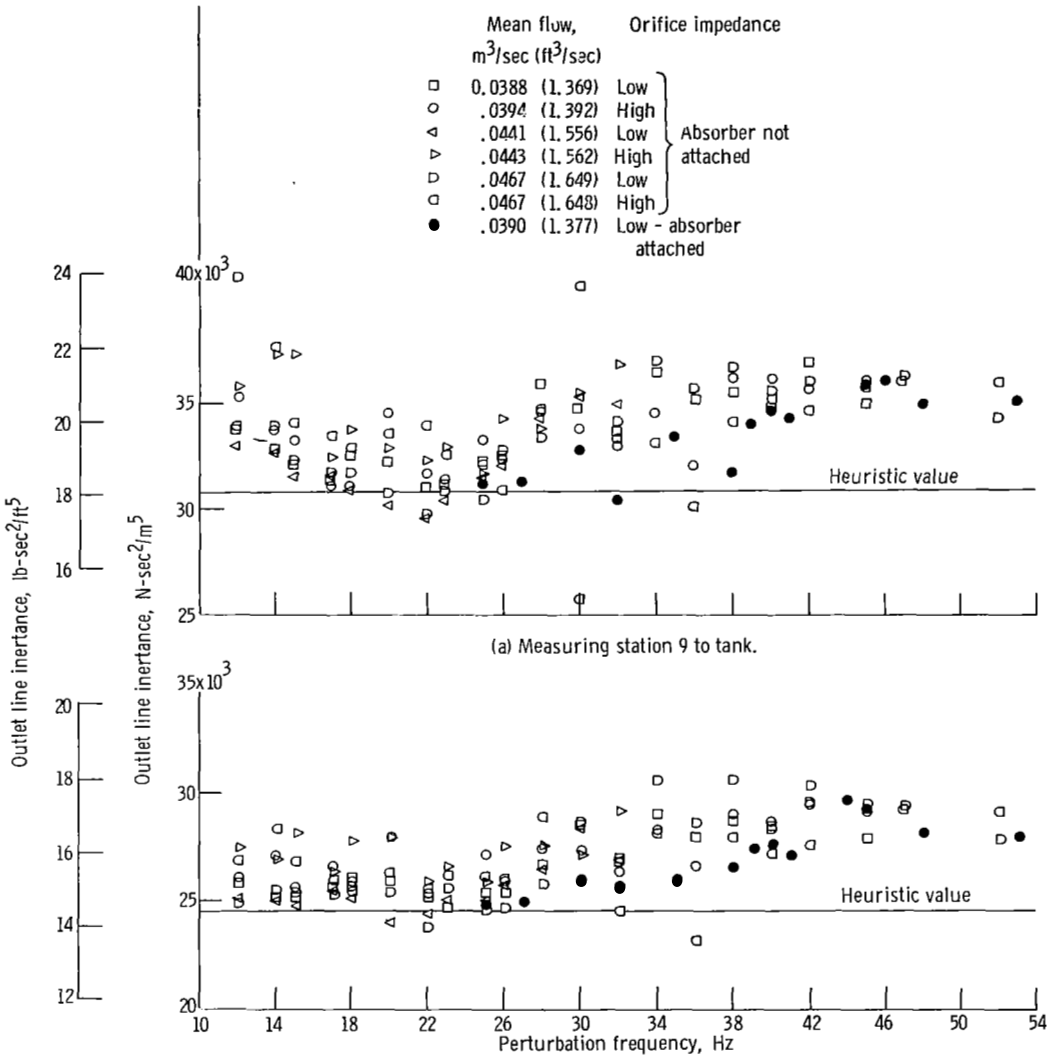

(a) Measuring station 9 to tank.

(b) Measuring station 10 to tank.

Figure 17. - Outlet line inertance as function of perturbation frequency. Pump inlet pressure for all runs, 482.63x10³ newtons per square meter (70 psi).

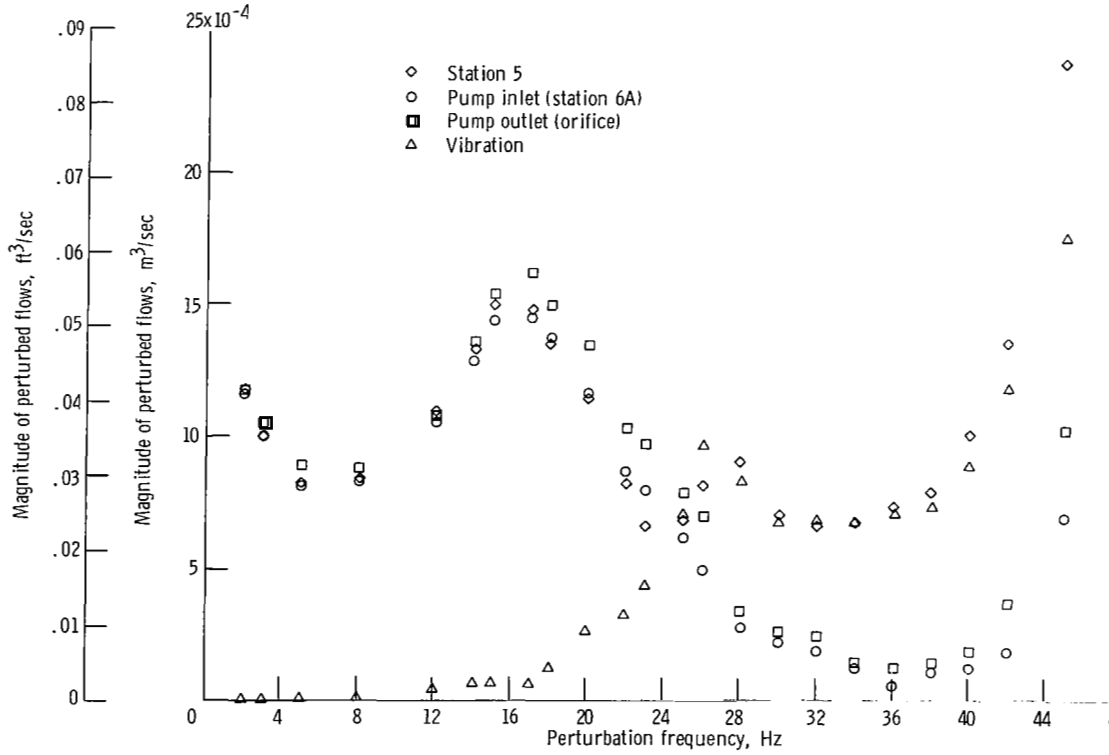

Figure 18. - Magnitude of perturbed flow as function of perturbation frequency.

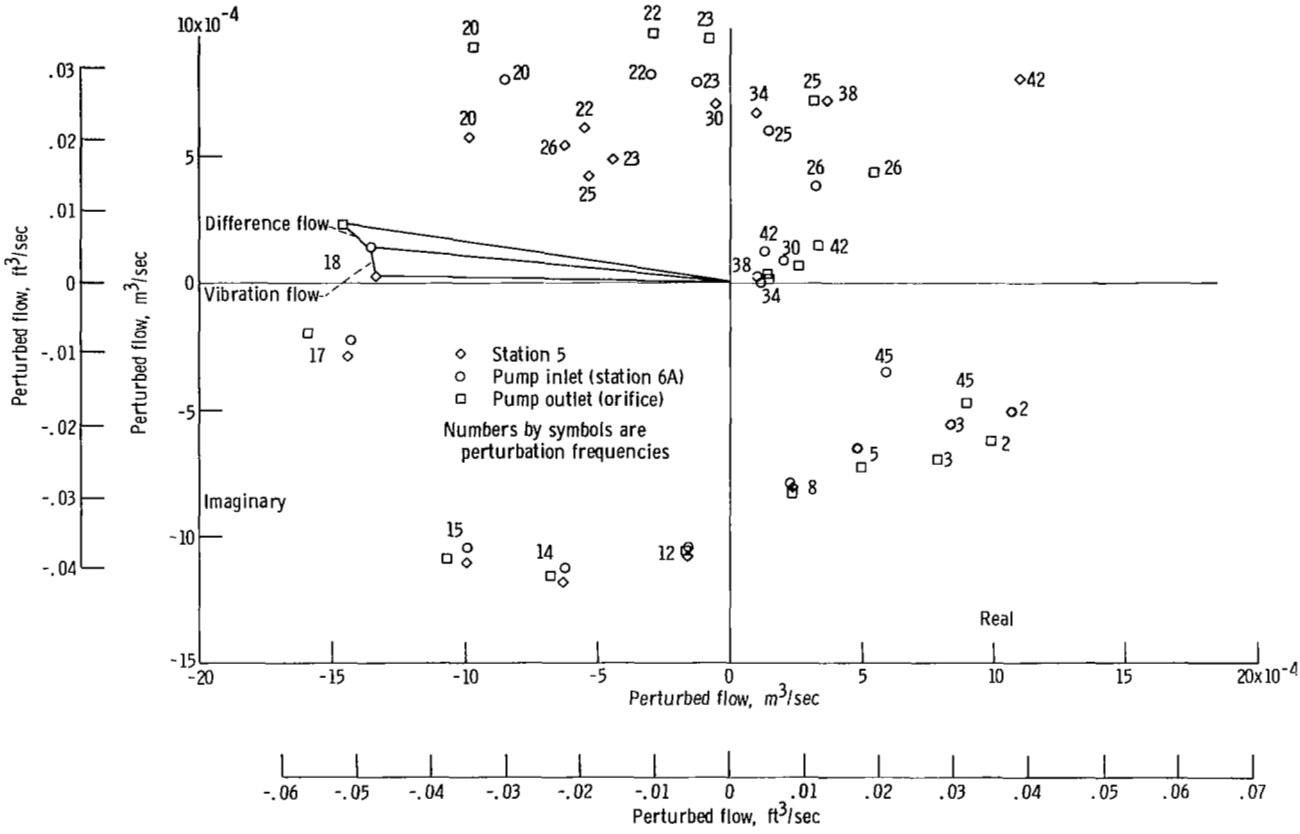

Figure 19. - Typical example of perturbed flow in polar coordinates.

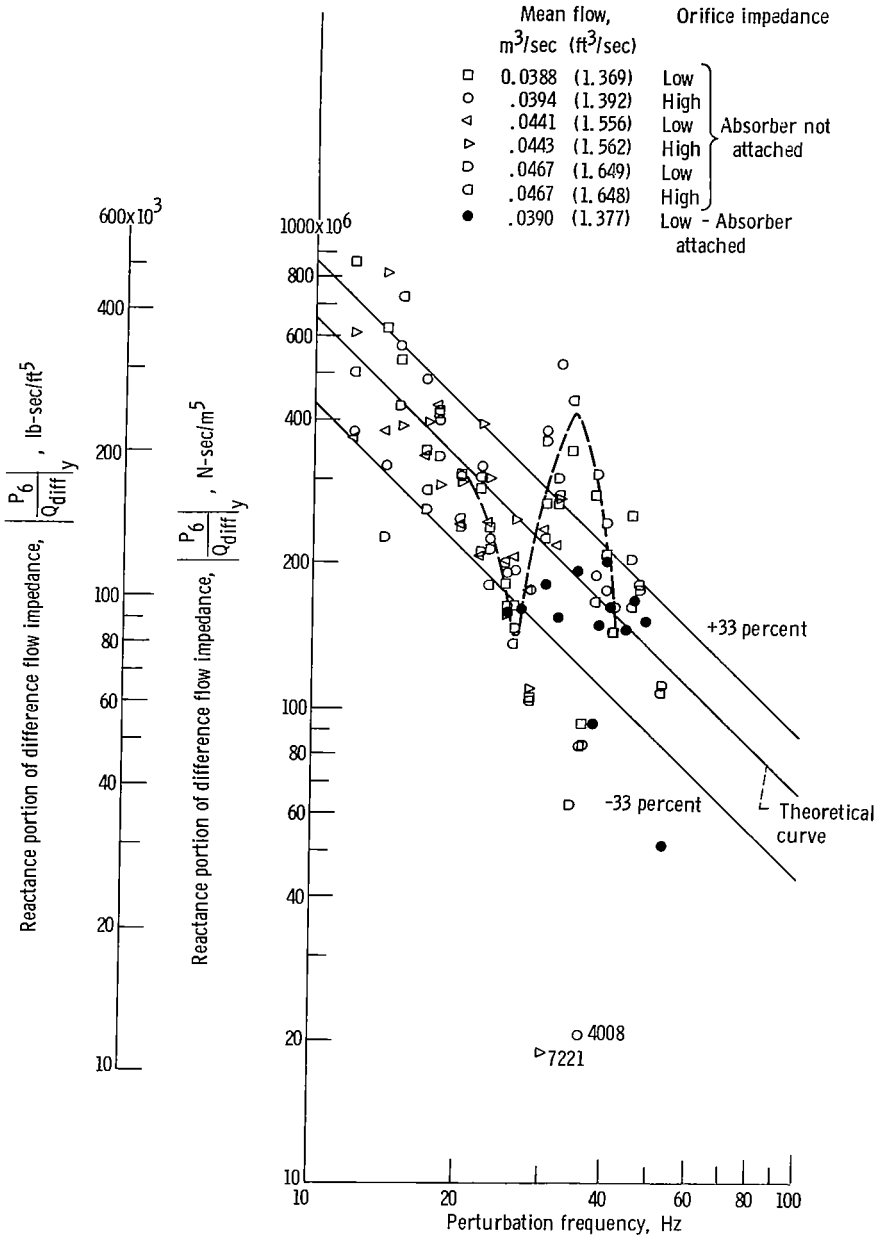

Figure 20. - Reactance portion of difference flow impedance as function of perturbation frequency. Pump inlet pressure for all runs, 482.63x10³ newtons per square meter (70 psi).

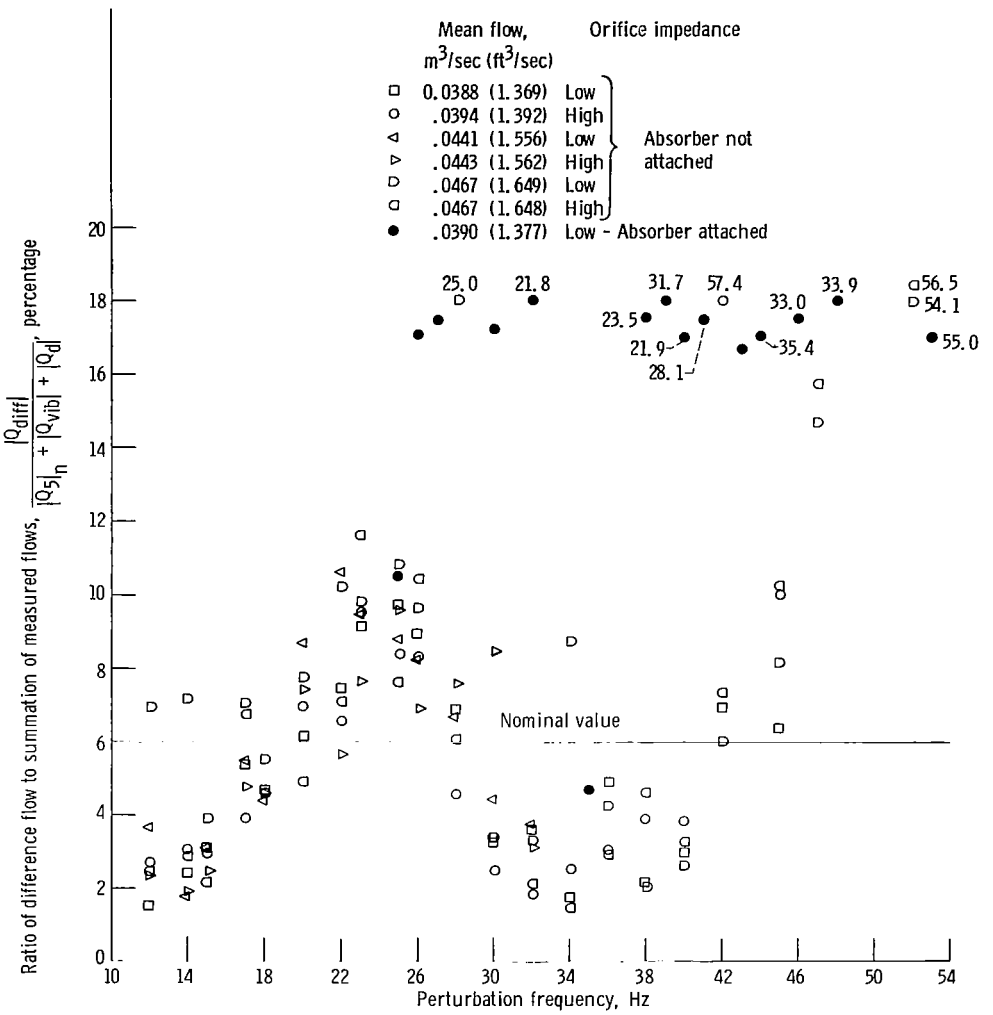

Figure 21. - Ratio of difference flow to summation of measured flows as function of perturbation frequency. Pump inlet pressure for all runs, 482.63×10^3 newtons per square meter (70 psi).

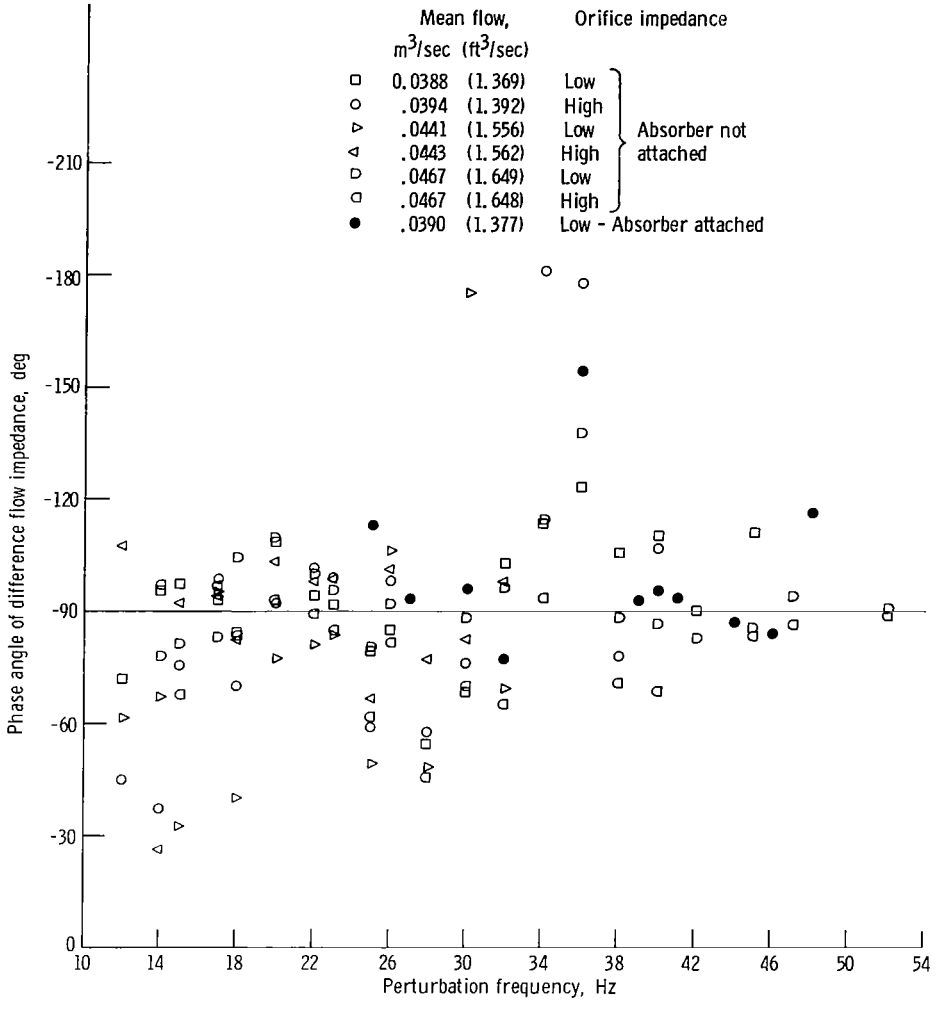

Figure 22. - Phase angle of difference flow impedance as function of perturbation frequency. Pump inlet pressure for all runs, 482.63×10^3 newtons per square meter (70 psi).

NASA-Langley, 1971 —— 12 E-4476

"The aeronautical and space activities of the United States shall be conducted so as to contribute . . . to the expansion of human knowledge of phenomena in the atmosphere and space. The Administration shall provide for the widest practicable and appropriate dissemination of information concerning its activities and the results thereof."

—NATIONAL AERONAUTICS AND SPACE ACT OF 1958

NASA SCIENTIFIC AND TECHNICAL PUBLICATIONS

TECHNICAL REPORTS: Scientific and technical information considered important, complete, and a lasting contribution to existing knowledge.

TECHNICAL NOTES: Information less broad in scope but nevertheless of importance as a contribution to existing knowledge.

TECHNICAL MEMORANDUMS: Information receiving limited distribution because of preliminary data, security classification, or other reasons.

CONTRACTOR REPORTS: Scientific and technical information generated under a NASA contract or grant and considered an important contribution to existing knowledge.

TECHNICAL TRANSLATIONS: Information published in a foreign language considered to merit NASA distribution in English.

SPECIAL PUBLICATIONS: Information derived from or of value to NASA activities. Publications include conference proceedings, monographs, data compilations, handbooks, sourcebooks, and special bibliographies.

TECHNOLOGY UTILIZATION PUBLICATIONS: Information on technology used by NASA that may be of particular interest in commercial and other non-aerospace applications. Publications include Tech Briefs, Technology Utilization Reports and Technology Surveys.

Details on the availability of these publications may be obtained from:

SCIENTIFIC AND TECHNICAL INFORMATION OFFICE

NATIONAL AERONAUTICS AND SPACE ADMINISTRATION

Washington, D.C. 20546